Table of contents

Welcome to the Complex Disordered Matter course! **2**
Overview . . . 2
Delivery and format . . . 3
Intended learning outcomes . . . 4
Contact details . . . 4
Questions and comments . . . 4

Recommended texts and literature **5**
Revision on thermodynamics and statistical mechanics . . . 5
Phase transitions and critical phenomena . . . 5
Stochastic dynamics . . . 5
Soft matter and glasses . . . 6

I Unifying concepts **7**

1 Introduction to phase behaviour and enhanced fluctuations **8**

2 Key concepts for phase transitions **11**
2.1 Observables and expectation values . . . 11
2.2 Correlations . . . 14
2.2.1 Spatial correlations . . . 14
2.2.2 Temporal correlations . . . 15

3 The approach to criticality **17**

4 The Ising model: the prototype model for a phase transition **20**
4.1 The 2D Ising model . . . 20
4.2 Exact solutions: the one dimensional Ising chain . . . 22
4.2.1 More general 1D spins systems: transfer matrix method . . . 25

5 Mean field theory and perturbation schemes **28**
5.1 Mean field solution of the Ising model . . . 28
5.2 Spontaneous symmetry breaking . . . 30
5.3 Phase diagram . . . 31

5.4 A closer look: critical exponents . . . 33
5.4.1 Zero H solution and the order parameter exponent . . . 33
5.4.2 Finite (but small) field solution: the susceptibility exponent . . . 34
5.5 Landau theory . . . 35
5.6 Shortcomings of mean field theory . . . 40

6 The Static Scaling Hypothesis 41
6.1 Experimental Verification of Scaling . . . 43
6.2 Computer simulation . . . 43

7 Universality and the Renormalisation Group Theory of Critical Phenomena 46
7.1 The critical point: A many length scale problem . . . 46
7.2 Methodology of the RG . . . 47
7.3 Universality and Scaling . . . 50
7.3.1 Fluid-magnet universality . . . 52
7.4 Near critical scaling . . . 52
7.5 Universality classes . . . 54
7.6 Critical exponents . . . 55
7.7 Finite-size scaling . . . 55
7.7.1 Finite-size scaling of the susceptibility . . . 56
7.7.2 Finite-size scaling of the order parameter . . . 57
7.8 Summary of main points . . . 57
7.9 Addendum: The effective coupling viewpoint of the renormalization group (non examinable) . . . 58
7.9.1 A simple example . . . 59
7.9.2 Universality and scaling . . . 63

8 Introduction to stochastic processes 66
8.1 The Master Equation . . . 66
8.2 From the Master Equation to the Diffusion Equation . . . 67
8.3 Consequences of time reversal symmetry . . . 71
8.3.1 Detailed balance . . . 71
8.3.2 Computer simulation . . . 72

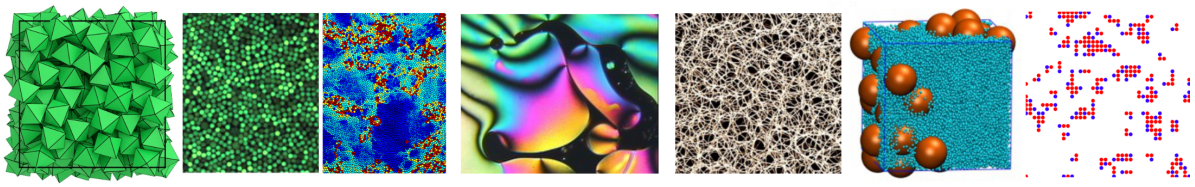
9 The Langevin Approach 75
9.1 The Random Walk and the Langevin equation . . . 75
9.2 Brownian Motion . . . 77
9.2.1 Noise Properties . . . 78
9.2.2 Solving the Langevin Equation (velocity) . . . 79
9.2.3 Mean-square velocity . . . 80
9.2.4 Mean-square displacement . . . 81
9.2.5 External Forces and Mobility . . . 84

9.2.6 Molecular Dynamics simulation of Brownian motion for a colloid particle in a liquid suspension 84

10 Dynamics of first order phase transitions: nucleation, growth and spinodal decomposition 90
10.1 Introduction to nucleation 90
10.2 Classical Nucleation Theory: Homogeneous Nucleation 91
10.2.1 Interpretation and Scaling Behaviour 93
10.3 Domain growth 94
10.4 Spinodal decomposition 94
10.4.1 Non-Conserved Order Parameter Dynamics (Model A) 95
10.4.2 Conserved Order Parameter Dynamics (Model B) 96
10.4.3 Schematic of Domain Growth in 2D Ising model 98
10.4.4 Dynamic Scaling Hypothesis 98
10.4.5 Summary of Growth Laws 99

Tools for understanding complex disordered matter 101
Ensembles and free energies 101
Microcanonical ensemble 101
Canonical ensemble 102
Grand canonical ensemble 103
Isothermal-isobaric ensemble 103
From free energies to observables 104

Welcome to the Complex Disordered Matter course!



Overview

This course introduces your to the theoretical, computational and experimental aspects of the physics of complex disordered matter.

Complex disordered matter is the study of wide range of systems like **polymers**, **colloids**, **glasses**, **gels**, and **emulsions**, which lack long-range order but exhibit intricate behaviour. Colloids, suspensions of microscopic particles in a fluid, are useful for studying disordered structures due to their observable dynamics. Similarly, polymer systems can form amorphous solids or glasses when densely packed or cooled, showing solid-like rigidity despite their disordered structure. These materials often undergo phase transitions, such as demixing and crystallisation, and near these transitions, they can display critical phenomena with extensive fluctuations and correlations.

These various systems are examples of **soft matter** systems. In such systems, the interplay between disorder, softness, and phase behavior leads to rich physical phenomena, particularly near critical points where even small changes in external conditions can trigger large-scale reorganisations and universal behaviour. Glasses, for instance, exhibit slow relaxation and memory effects, while colloidal systems may crystallize, phase separate, or become jammed depending on particle interactions and concentration. Understanding such behaviors involves studying how microscopic interactions and thermal fluctuations influence macroscopic properties, especially in non-equilibrium conditions. Through techniques like scattering, microscopy, rheology, and simulation, one can explore how disordered soft materials respond to stress, age, or undergo transitions—insights that are vital for applications in materials design, biotechnology, and beyond.

This course is organized into three interconnected parts, each offering a distinct perspective on the study of complex disordered matter.

- **Part 1: Unifying concepts** (Nigel Wilding) introduces the theoretical framework for rationalising complex disordered matter which is grounded in statistical mechanics and thermodynamics. We emphasize the theory of phase transitions, thermal fluctuations, critical phenomena, and stochastic dynamics—providing the essential theoretical tools needed to describe and predict the behavior of soft and disordered systems.

- **Part 2: Complex disordered matter** (Francesco Turci) explores the phenomenology of key examples of complex disordered soft matter systems, including colloids, polymers, liquid crystals, glasses, gels, and active matter. These systems will be analyzed using the theoretical concepts introduced in Part 1, highlighting how disorder, interactions, and fluctuations shape their macroscopic behavior.
- **Part 3: Experimental techniques** (Alexis Darras) focuses on the methods of microscopy, and scattering via x-rays, neutrons and light that are used to study complex disordered matter, offering insight into how their properties are measured and understood in real-world contexts.

In addition to theory and experiment, computer simulation plays a central role in soft matter research. This course includes a substantial coursework component consisting of a computational project. This exercise will allow you to apply state-of-the-art simulation techniques to investigate the complex behavior of disordered systems, bridging theory and observation through hands-on exploration.

Delivery and format

- Detailed e-notes (accessible via Blackboard) can be viewed on a variety of devices. Pdf is also available.
- We will give 'traditional' lectures (Mondays, Wednesdays, Fridays) in which we use slides to summarise and explain the lecture content. Questions are welcome (within reason…)
- Try to read ahead in the notes, then come to lectures, listen to the explanations and then reread the notes.
- Rewriting the notes or slides to express your own thoughts and understanding, or annotating a pdf copy can help wire the material into your own way of thinking.
- There are problem classes (Thursdays) where you can try problem sheets and seek help. Lecturers may go over some problems with the class, treating them as worked examples.

- The navigation bar on the left will allow you to access the lecture notes and problem sets.

Intended learning outcomes

The course will

- Introduce you to the qualitative features of a range of complex and disordered systems and the experimental techniques used to study them.
- Introduce you to a range of model systems and theoretical techniques used to elucidate the physics of complex disordered matter.
- Provide you with elementary computational tools to model complex disordered systems numerically and predict their properties.
- Allow you to apply your physics background to understand a variety of systems of interdisciplinary relevance.
- Connect with the most recent advances in the research on complex disordered matter.

Contact details

The course will be taught by

- Prof Nigel B. Wilding (unit director): nigel.wilding@bristol.ac.uk
- Dr Francesco Turci: F.Turci@bristol.ac.uk
- Dr Alexis Darras: alexis.darras@bristol.ac.uk

Questions and comments

If you have any questions about the course, please don't hesitate to contact the relevant lecturer, either by email (see above) or in a problems class. Should you find any errors or mistakes or something which isn't clear, please let us know by email, or fill in this anonymous form:

> Submit an error/mistake/query

Recommended texts and literature

One motivation for supplying you with detailed notes for this course course is the absence of a single wholly ideal text book. However, it should be stressed that while these notes approach (in places) the detail of a book, the notes are not fully comprehensive and should be regarded as the 'bare bones' of the course, to be fleshed out via your own reading and supplementary note taking.

Revision on thermodynamics and statistical mechanics

See your year two Thermal Physics notes. Also

- **F. Mandl: Statistical Physics**

Phase transitions and critical phenomena

A good book at the right level for the phase transitions and critical phenomena part of the course is

- **J.M. Yeomans: Statistical Mechanics of Phase Transitions**

A good book covering all aspects of this part of the course including non-equilibrium systems is

- **D. Chandler: Introduction to Modern Statistical Mechanics**

You might also wish to dip into the introductory chapters of the following more advanced texts

- **N Goldenfeld: Lectures on Phase Transitions and the Renormalization Group**
- **J.J. Binney, N.J. Dowrick, A.J.Fisher and M.E.J. Newman: The Theory of Critical Phenomena**

Stochastic dynamics

- **N.G. van Kampen: Stochastic processess in Physics and Chemistry**

Soft matter and glasses

The best overall text for part 2 of the course is:

- **R.A.L Jones, Soft Condensed Matter**.

Additionally, the following more specialised texts (which include information on experimental techniques) might be useful.

Colloids

- **D.F.Evans, H.Wennerström: The Colloidal Domain - Where Physics, Chemistry, Biology, and Technology Meet**
- **R.J.Hunter: Introduction to Modern Colloid Science**
- **W.B.Russel, D.A.Saville, W.R.Schowalter: Colloidal Dispersions**
- **D.H.Everett: Basic Principles of Colloid Science**

Polymers and surfactants

- **R.J. Young and P.A. Lovell: Introduction to polymers**
- **M. Doi: Introduction to polymer physics**
- **J.Israelachvili, Intermolecular and Surface Forces**

Glasses

- **J. Zarzycki; Glasses and the vitreous state**

Part I

Unifying concepts

1 Introduction to phase behaviour and enhanced fluctuations

A phase transition can be defined as a macroscopic rearrangment of the internal constituents of a system in response to a change in the thermodynamic conditions to which they are subject. A wide variety of physical systems undergo such transitions. Understanding the properties of phase transitions is fundamental to the study of soft and complex matter, as these systems often exhibit rich and subtle transformations between different states of organization. Whether in colloidal suspensions, polymer blends, liquid crystals, or biological materials, phase transitions underpin a wide range of physical behaviours, from self-assembly and pattern formation to critical phenomena and dynamical arrest. By analysing how macroscopic phases emerge from microscopic interactions and external conditions, one gains crucial insight into the principles that govern structure, stability, and functionality in these intricate systems. As such, an understanding of phase transitions not only enriches theoretical understanding but also informs practical applications across materials science, biophysics, and nanotechnology. For these reasons we will devote a large proportion of this course to the study of phase transitions.

Two classic examples of systems displaying phase transitions are the ferromagnet and fluid systems. For the magnet, a key observable is the magnetisation defined as the magnetic moment per spin, given by $m = M/N$, with N the number of spins. m can be positive or negative, dependent on whether the spins are aligned 'up' or 'down'. As the temperature of a ferromagnet is increased, its net magnetisation $|m|$ is observed to decrease smoothly, until at a certain temperature known as the critical temperature, T_c, it vanishes altogether (see left part of Figure 1.1). We define the magnetisation to be the *order parameter* of this phase transition.

One can also envisage applying a magnetic field H to the system which, depending on its sign (i.e. whether it is aligned (positive) or anti-aligned (negative) relative to the magnetisation axis), favours up or down spin states respectively, as shown schematically in Figure 1.1 (right part). Changing the sign of the magnetic field H for $T < T_c$ leads to a phase transition chacterised by a discontinuous jump in m. We shall explore this behaviour in more detail in section 5.

Similarly, a change of state from liquid to gas can be induced in a fluid system (though not in an ideal gas) simply by raising the temperature. Typically the liquid-vapour transition is abrupt, reflecting the large number density difference between the states either side of the transition. However the abruptness of this transition can be reduced by applying pressure. At

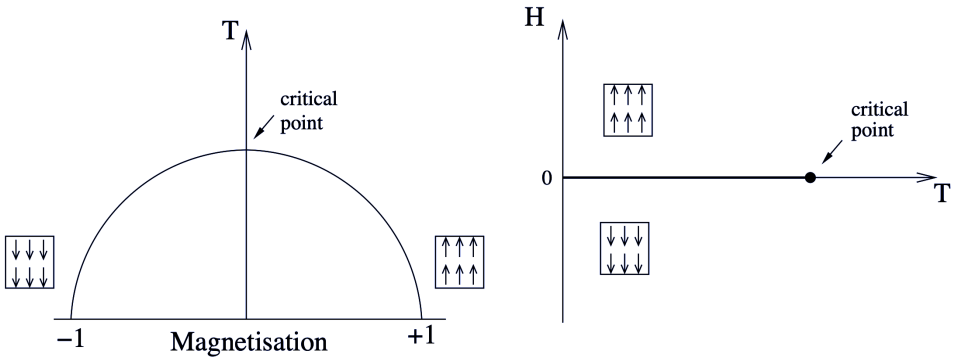


Figure 1.1: Phase diagram of a simple magnet (schematic). Left: magnetisation as a function of temperature for zero applied magnetic field, $H = 0$. Right: Applying a magnetic field that is aligned or antialigned with the direction of the magnetisation leads to a phase transition. The $H = 0$ axis at $T < T_c$ is the coexistence curve for which positive and negative magnetisations are equally likely.

one particular pressure and temperature the discontinuity in the density difference between the two states vanishes and the two phases coalesce. These conditions of pressure and temperature serve to locate the critical point for the fluid. We define the density difference $\rho_{liq} - \rho_{vap}$ to be the order parameter for the liquid-gas phase transition. We shall meet order parameters for other, more complex, systems in section 5,

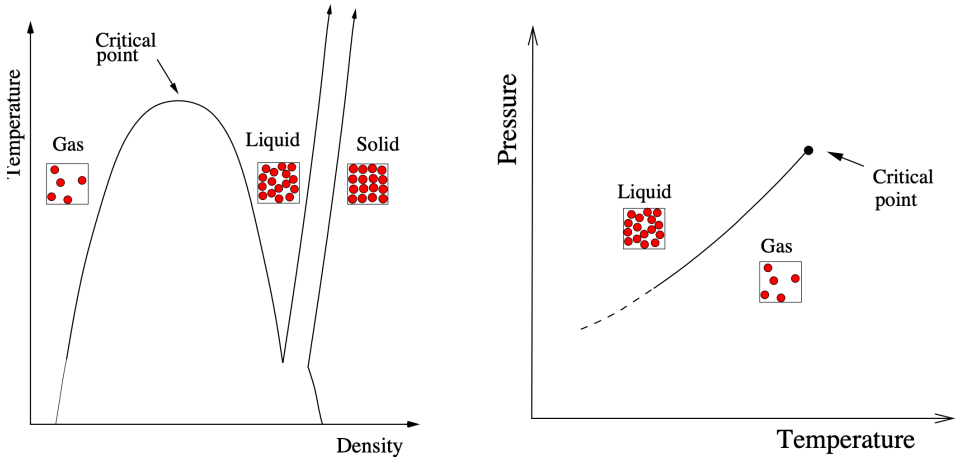


Figure 1.2: Phase diagram of a simple fluid (schematic)

In the vicinity of a critical point, a system displays a host of remarkable behaviors known as *critical phenomena*. Chief among these is the divergence of thermal response functions—such as specific heat, compressibility, or magnetic susceptibility—which signal an enhanced sensitivity to external perturbations. These singularities arise from the emergence of large-scale cooperative interactions among the system's microscopic constituents, as measured by

a diverging *correlation length* (see Chapter 2). One visually striking manifestation of this is *critical opalescence*, particularly observed in fluids like CO_2. As carbon dioxide nears its critical temperature and pressure, the distinction between its liquid and gas phases vanishes, giving rise to huge fluctuations in density. These fluctuations scatter visible light, rendering the fluid milky or opalescent. This scattering effect directly reflects the long-range correlations developing within the fluid. The movie below illustrates the effect as the critical temperature of CO_2 is approached from above. Note the appearence of a liquid-vapour interface (meniscus) as the system enters the two-phase region.

Movies/critical_point_1.mp4

The recalcitrant problem posed by the critical region is how best to incorporate such collective effects within the framework of a rigorous mathematical theory that affords both physical insight and quantitative explanation of the observed phenomena. This matter has been (and still is!) the subject of intense theoretical activity.

The importance of the critical point stems largely from the fact that many of the phenomena observed in its vicinity are believed to be common to a whole range of apparently quite disparate physical systems. Systems such as liquid mixtures, superconductors, liquid crystals, ferromagnets, antiferromagnets and molecular crystals may display identical behaviour near criticality. This observation implies a profound underlying similarity among physical systems at criticality, regardless of many aspects of their distinctive microscopic nature. These ideas have found formal expression in the so-called 'universality hypothesis' which, since its inception in the 1970s, has enjoyed considerable success.

In the next few lectures, principal aspects of the contemporary theoretical viewpoint of phase transitions and critical phenomena will be reviewed. Mean field theories of phase transitions will be discussed and their inadequacies in the critical region will be exposed. The phenomenology of the critical region will we described including power laws, critical exponents and their relationship to scaling phenomena. These will be set within the context of the powerful renormalisation group technique. The notion of universality as a phenomenological hypothesis will be introduced and its implications for real and model systems will be explored. Finally, the utility of finite-size scaling methods for computer studies of critical phenomena will be discussed, culminating in the introduction of a specific technique suitable for exposing universality in model systems. Thereafter we will consider some foundational concepts in the dynamics of complex disordered matter. We shall look at the processes by which one phase transform into another and introduce differential equations that allow us to deal with the inherent stochasticity of thermal systems. The wider applicability of these unifying concepts to complex disordered systems such as colloids, polymers, liquid crystals and glasses will be covered in part 2 of the course.

2 Key concepts for phase transitions

2.1 Observables and expectation values

In seeking to describe phase transition and critical phenomena, it is useful to have a quantitative measure of the difference between the phases: this is the role of the *order parameter*, Q. In the case of the fluid, the order parameter is taken as the difference between the densities of the liquid and vapour phases. In the ferromagnet it is taken as the magnetisation. As its name suggest, the order parameter serves as a measure of the kind of orderliness that sets in when the temperature is cooled below a critical temperature.

Our first task is to give some feeling for the principles which underlie the ordering process. Referring back to **?@sec-canonical**, the probability p_a that a physical system at temperature T will have a particular microscopic arrangement (alternatively referred to as a 'configuration' or 'state'), labelled a, of energy E_a is

$$p_a = \frac{1}{Z} e^{-E_a/k_B T} \tag{2.1}$$

The prefactor Z^{-1} is the *partition function*: since the system must always have *some* specific arrangement, the sum of the probabilities p_a must be unity, implying that

$$Z = \sum_a e^{-E_a/k_B T} \tag{2.2}$$

where the sum extends over all possible microscopic arrangements.

These equations assume that physical system evolves rapidly (on the timescale of typical observations) amongst all its allowed arrangements, sampling them with the probabilities Equation 2.1 the expectation value of any physical observable O will thus be given by averaging O over all the arrangements a, weighting each contribution by the appropriate probability:

$$\overline{O} = \frac{1}{Z} \sum_a O_a e^{-E_a/k_B T} \tag{2.3}$$

Sums like Equation 2.3 are not easily evaluated because the number of terms grows exponentially in the system size. Nevertheless, some important insights follow painlessly. Consider

the case where the observable of interest is the order parameter, or more specifically the magnetisation of a ferromagnet.

$$Q = \frac{1}{Z} \sum_a Q_a e^{-E_a/k_B T} \tag{2.4}$$

It is clear from Equation 2.1 that at very low temperature the system will be overwhelmingly likely to be found in its minimum energy arrangements (ground states). For the ferromagnet, these are the fully ordered spin arrangements having magnetisation $+1$, or -1.

Now consider the high temperature limit. The enhanced weight that the fully ordered arrangement carries in the sum of Equation 2.4 by virtue of its low energy, is now no longer sufficient to offset the fact that arrangements in which Q_a has some intermediate value, though each carry a smaller weight, are vastly greater in number. A little thought shows that the arrangements which have essentially zero magnetisation (equal populations of up and down spins) are by far the most numerous. At high temperature, these disordered arrangements dominate the sum in Equation 2.4 and the order parameter is zero.

The competition between energy-of-arrangements weighting (or simply 'energy') and the 'number of arrangements' weighting (or 'entropy') is then the key principle at work here. The distinctive feature of a system with a critical point is that, in the course of this competition, the system is forced to choose amongst a number of macroscopically different sets of microscopic arrangements.

Finally in this section, we note that the probabilistic (statistical mechanics) approach to thermal systems outlined above is completely compatible with classical thermodynamics. Specifically, the bridge between the two disciplines is provided by the following equation

$$F = -k_B T \ln Z \tag{2.5}$$

where F is the "Helmholtz free energy". All thermodynamic observables, for example the order parameter Q, and response functions such as the specific heat or magnetic susceptibility are obtainable as appropriate derivatives of the free energy. For instance, utilizing Equation 2.2, one can readily verify (try it as an exercise!) that the average internal energy is given by

$$\overline{E} = -\frac{\partial \ln Z}{\partial \beta},$$

where $\beta = (k_B T)^{-1}$.

The relationship between other thermodynamic quantities and derivatives of the free energy are given in fig. Figure 2.1

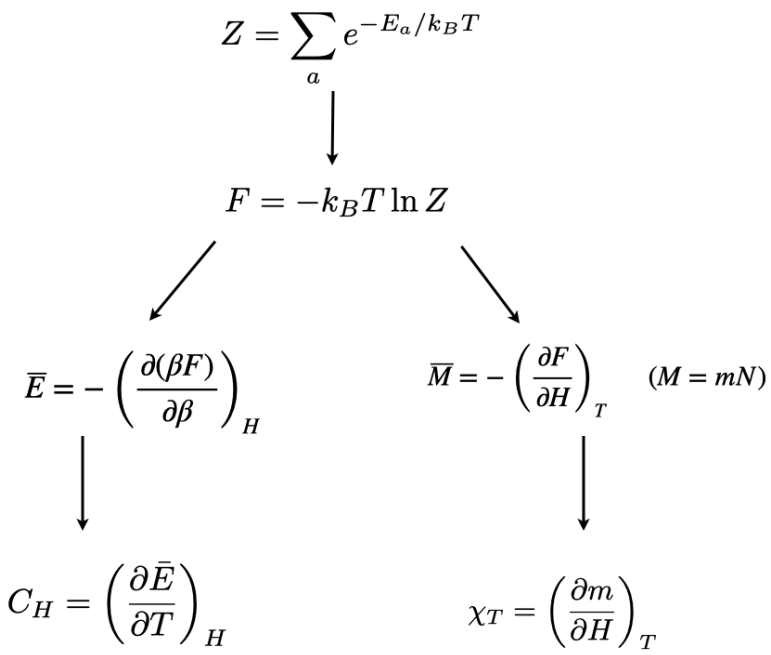


Figure 2.1: Relationships between the partition function and thermodynamic observables

2.2 Correlations

2.2.1 Spatial correlations

The two-point connected correlation function measures how fluctuations at two spatial points are statistically related. For a scalar field $\phi(\vec{R})$, which could represent eg. the local magnetisation m in a magnet at position vector $\vec{R}$, or the local particle number density ρ in a fluid, it is defined as:

$$C(r) = \langle \phi(\vec{R})\phi(\vec{R}+\vec{r})\rangle - \langle \phi(\vec{R})\rangle^2,$$

where $\langle\cdot\rangle$ denotes an ensemble or spatial average over all $\vec{R}$, and $r = |\vec{r}|$ is the spatial separation between the two points.

$C(r)$ quantifies the spatial extent over which field values are correlated and in homogeneous and isotropic systems, it depends only on the separation r.

If $C(r)$ decays quickly, we say that correlations are short-ranged. Typically this occurs well away from criticality and takes the form of exponential decay

$$C(r) \sim e^{-r/\xi}$$

where the correlation length ξ is the characteristic scale over which correlations decay.

Near a critical point $C(r)$ decays more slowly - in a power-law fashion - and correlations are long-ranged.

$$C(r) \sim r^{-(d-2+\eta)}$$

where d is the spatial dimension and η is a critical exponent.

In isotropic fluids and particle systems, a closely related and more directly measurable quantity (particularly in simulations) is the **radial distribution function** $g(r)$, which describes how particle density varies as a function of distance from a reference particle. For such systems, the two-point correlation function of the number density field $\rho(\vec{r})$ is related to $g(r)$ as follows:

$$g(r) = 1 + \frac{C(r)}{\rho^2},$$

where ρ is the average number density. This relation shows that $g(r)$ encodes the same spatial correlations as $C(r)$, but in a form that is more natural for discrete particle systems. Note that by definition $g(r) \to 1$ in the absence of correlations ie. when $C(r) = 0$. This is typically the case for $r \gg \xi$.

Experimentally one doesn't typically have direct access to $C(r)$, but rather its Fourier transform known as the **structure factor**

$$S(k) = \int d^d r \, e^{-i\vec{k}\cdot\vec{r}} \, C(r),$$

where k is the scattering wavevector and $d^d r$ refers to the elemental volume (eg. $d^3 r$ in three dimensions).

In equilibrium:

- For short-range correlations (finite ξ), $S(k)$ typically has a Lorentzian form:

$$S(k) \sim \frac{1}{k^2 + \xi^{-2}}.$$

- At criticality (where $\xi \to \infty$), $S(k)$ follows a power law:

$$S(k) \sim k^{-2+\eta}.$$

This relation enables the extraction of ξ from experimental or simulation data, especially via scattering techniques.

2.2.2 Temporal correlations

Consider a thermodynamic variable x with zero mean that fluctuates over time. Examples include the local magnetization in a magnetic system or the local density in a fluid. Here, x represents a deviation from the average value — a fluctuation.

We're interested in how such fluctuations are correlated over time when the system is in thermal equilibrium. For instance, if x is positive at some time t, it's more likely to remain positive shortly after.

These temporal correlations are characterized by the two-time correlation function (also known as an auto-correlation function):

$$\langle x(\tau) x(\tau + t) \rangle$$

In equilibrium, the correlation function does not evolve with time, so must be independent of the starting time τ. Therefore, we define:

$$\langle x(\tau) x(\tau + t) \rangle = M_{xx}(t)$$

That is, $M_{xx}(t)$ depends only on the time difference t.

We typically expect $M_{xx}(t)$ to decay exponentially over a characteristic correlation time t_c:

$$M_{xx}(t) \sim \exp(-t/t_c)$$

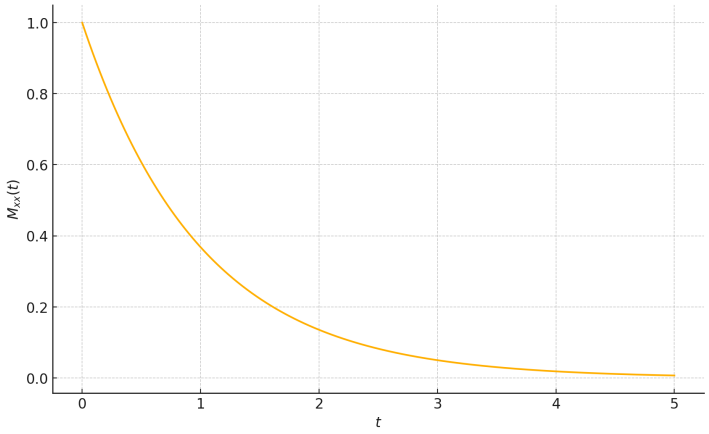


Figure 2.2: Sketch of $M_{xx}(t)$ against t

This exponential decay reflects how the memory of fluctuations fades with time.

Now consider two different fluctuating variables, x and y (e.g., local magnetizations at different positions). Their cross-correlation function is defined as:

$$\langle x(\tau)y(\tau + t)\rangle = M_{xy}(t)$$

This defines the elements of a dynamic correlation matrix, of which $M_{xx}(t)$ is the diagonal.

3 The approach to criticality

It is a matter of experimental fact that the approach to criticality in a given system is characterized by the divergence of various thermodynamic observables. Let us remain with the archetypal example of a critical system, the ferromagnet, whose critical temperature will be denoted as T_c. For temperatures close to T_c, the magnetic response functions (the magnetic susceptibility χ and the specific heat) are found to be singular functions, diverging as a *power* of the reduced (dimensionless) temperature $t \equiv (T - T_c)/T_c$:-

$$\chi \equiv \frac{\partial M}{\partial H} \propto t^{-\gamma} \quad (H = 0) \tag{3.1}$$

(where $M = mN$),

$$C_H \equiv \frac{\partial E}{\partial T} \propto t^{-\alpha} \quad (H = 0) \tag{3.2}$$

Another key quantity is the correlation length ξ, which measures the distance over which fluctuations of the magnetic moments are correlated. This is observed to diverge near the critical point with an exponent ν.

$$\xi \propto t^{-\nu} \quad (T > T_c,\ H = 0) \tag{3.3}$$

Similar power law behaviour is found for the order parameter Q (in this case the magnetisation) which vanishes in a singular fashion (it has infinite gradient) as the critical point is is approached as a function of temperature:

$$m \propto t^{\beta} \quad (T < T_c,\ H = 0) \tag{3.4}$$

(here the symbol β, is not to be confused with $\beta = 1/k_B T$– this unfortunately is the standard notation.)

Finally, as a function of magnetic field:

$$m \propto h^{1/\delta} \quad (T = T_c,\ |H| > 0). \tag{3.5}$$

with $h = H/k_B T_c$, the reduced magnetic field (note here is is assumed that H is expressed in energy units to make h dimensionless).

As examples, the behaviour of the magnetisation and correlation length are plotted in Figure 3.1 as a function of t.

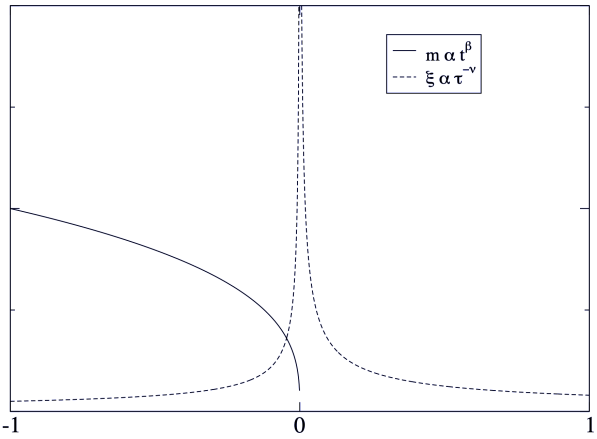


Figure 3.1: Singular behaviour of the correlation length and order parameter in the vicinity of the critical point as a function of the reduced temperature t.

The quantities $\gamma, \alpha, \nu, \beta$ in the above equations are known as critical exponents. They serve to control the rate at which the various thermodynamic quantities change on the approach to criticality.

Remarkably, the form of singular behaviour observed at criticality for the example ferromagnet also occurs in qualitatively quite different systems such as the fluid. All that is required to obtain the corresponding power law relationships for the fluid is to substitute the analogous thermodynamic quantities in to the above equations. Accordingly the magnetisation order parameter is replaced by the density difference $\rho_{liq} - \rho_{gas}$ while the susceptibility is replaced by the isothermal compressibility and the specific heat capacity at constant field is replaced by the specific heat capacity at constant volume. The approach to criticality in a variety of qualitatively quite different systems can therefore be expressed in terms of a set of critical exponents describing the power law behaviour for that system (see the book by Yeomans for examples).

Even more remarkable is the experimental observation that the values of the critical exponents for a whole range of fluids and magnets (and indeed many other systems with critical points) are *identical*. This is the phenomenon of *universality*. It implies a deep underlying physical similarity between ostensibly disparate critical systems. The principal aim of theories of critical point phenomena is to provide a sound theoretical basis for the existence of power law behaviour, the factors governing the observed values of critical exponents and the universality phenomenon. Ultimately this basis is provided by the Renormalisation Group (RG) theory, for which K.G. Wilson was awarded the Nobel Prize in Physics in 1982.

More about the scientists mentioned in this chapter:

Kenneth Wilson

4 The Ising model: the prototype model for a phase transition

In order to probe the properties of the critical region, it is common to appeal to simplified model systems whose behaviour parallels that of real materials. The sophistication of any particular model depends on the properties of the system it is supposed to represent. The simplest model to exhibit critical phenomena is the two-dimensional Ising model of a ferromagnet. Actual physical realizations of 2-d magnetic systems do exist in the form of layered ferromagnets such as K_2CoF_4, so the 2-d Ising model is of more than just technical relevance.

4.1 The 2D Ising model

The 2-d spin-$\frac{1}{2}$ Ising model envisages a regular arrangement of magnetic moments or 'spins' on an infinite plane. Each spin can take two values, $+1$ ('up' spins) or -1 ('down' spins) and is assumed to interact with its nearest neighbours according to the Hamiltonian

$$H_I = -J \sum_{<ij>} s_i s_j - H \sum_i s_i \tag{4.1}$$

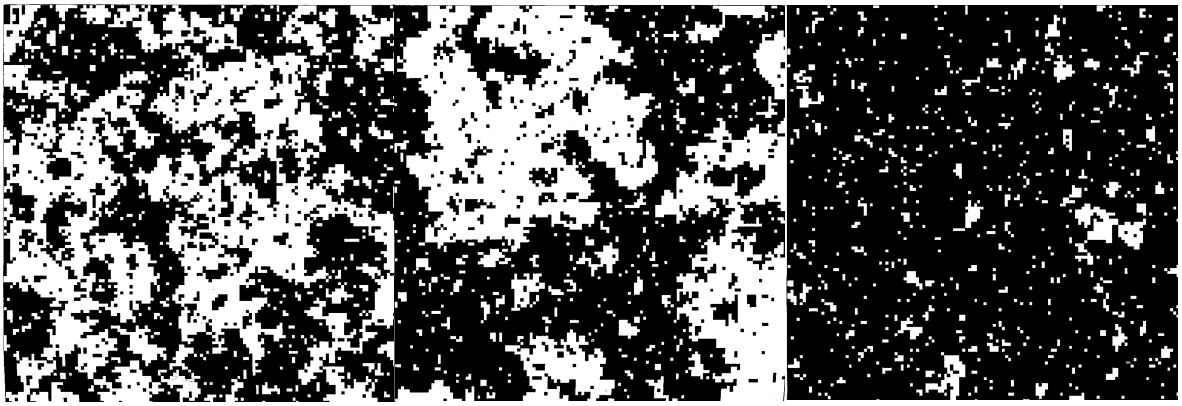
where $J > 0$ measures the strength of the coupling between spins and the sum extends over nearest neighbour spins s_i and s_j, i.e it is a sum of the bonds of the lattice. H is a magnetic field term which can be positive or negative (although for the time being we will set it equal to zero). The order parameter is simply the average magnetisation:

$$m = \frac{1}{N} \langle \sum_i s_i \rangle \ ,$$

where $\langle \cdot \rangle$ means an average over typical configurations corresponding to the prescribed value of $J/k_B T$.

The fact that the Ising model displays a phase transition was argued in Chapter 2. Thus at low temperatures for which there is little thermal disorder, there is a preponderance of aligned spins and hence a net spontaneous magnetic moment (ie. the system is ferromagnetic). As the temperature is raised, thermal disorder increases until at a certain temperature T_c, entropy drives the system through a continuous phase transition to a disordered spin arrangement

with zero net magnetisation (ie. the system is paramagnetic). These trends are visible in configurational snapshots from computer simulations of the 2D Ising model (see Figure 4.1). Although each spin interacts only with its nearest neighbours, the phase transition occurs due to cooperative effects among a large number of spins.



(a) $T = 1.2T_c$ (b) $T = T_c$ (c) $T = 0.95T_c$

Figure 4.1: Configurations of the 2d Ising model. The patterns depict typical arrangements of the spins (white=+1, black=−1) generated in a computer simulation of the Ising model on a square lattice of $N = 512$ sites, at temperatures (from left to right) of $T = 1.2T_c$, $T = T_c$, and $T = 0.95T_c$. In each case only a portion of the system containing 128 sites in shown. The typical island size is a measure of the correlation length ξ: the excess of black over white (below T_c is a measure of the order parameter.

An interactive Monte Carlo simulation of the Ising model demonstrates the phenomenology, By altering the temperature you will be able to observe for yourself how the typical spin arrangements change as one traverses the critical region. Pay particular attention to the configurations near the critical point. They have very interesting properties. We will return to them later!

Although the 2-d Ising model may appear at first sight to be an excessively simplistic portrayal of a real magnetic system, critical point universality implies that many physical observables such as critical exponents are not materially influenced by the actual nature of the microscopic interactions. The Ising model therefore provides a simple, yet *quantitatively* accurate representation of the critical properties of a whole range of real magnetic (and indeed fluid) systems. This universal feature of the model is largely responsible for its ubiquity in the field of critical phenomena. We shall explore these ideas in more detail later in the course.

4.2 Exact solutions: the one dimensional Ising chain

One might well ask why the 2D Ising model is the simplest model to exhibit a phase transition. What about the one-dimensional Ising model (ie. spins on a line)? In fact in one dimension, the Ising model can be solved exactly. It turns out that the system is paramagnetic for all $T > 0$, so there is no phase transition at any finite temperature. To see this, consider the ground state of the system in zero external field. This will have all spins aligned the same way (say up), and hence be ferromagnetic. Now consider a configuration with a various "domain walls" dividing spin up and spin down regions:

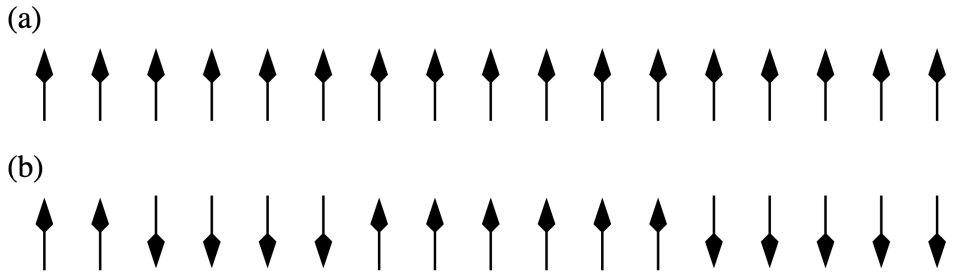


Figure 4.2: (a) Schematic of an Ising chain at $T = 0$. (b) At a small finite temperature the chain is split into domains of spins ordered in the same direction. Domains are separated by notional domain "walls", which cost energy $\Delta = 2J$. Periodic boundary conditions are assumed.

Instead of considering the underlying spin configurations, we shall describe the system in terms of the statistics of its domain walls. The energy cost of a wall is $\Delta = 2J$, independent of position. Domain walls can occupy the bonds of the lattice, of which there are $N - 1$. Moreover, the walls are noninteracting, except that you cannot have two of them on the same bond. (Check through these ideas if you are unsure.)

In this representation, the partition function involves a count over all possible domain wall arrangements. Since the domain walls are non interacting (eg it doesn't cost energy for one to move along the chain) they can be treated as independent. Independent contributions to the partition function simply multiply. So we can calculate Z by considering the partition function associated with a single domain wall being present or absent on some given bond, and then simply raise to the power of the number of bonds:

$$Z = Z_1^{N-1}$$

where

$$Z_1 = e^{\beta J} + e^{\beta(J-\Delta)} = e^{\beta J}(1 + e^{-\beta\Delta})$$

is the domain wall partition function for a single bond and represent the sum over the two possible states: domain wall absent or present. Then the free energy per bond of the system is

$$\beta f \equiv \beta F/(N-1) = -\ln Z_1 = -\beta J - \ln(1+e^{-\beta\Delta})$$

The first term on the RHS is simply the energy per spin of the ferromagnetic (ordered) phase, while the second term arises from the free energy of domain walls. Clearly for any finite temperature (ie. for $\beta < \infty$), this second term is finite and negative. Hence the free energy will always be lowered by having a finite concentration of domain walls in the system. Since these domain walls disorder the system, leading to a zero average magnetisation, the 1D system is paramagnetic for all finite temperatures. *Exercise*: Explain why this argument works only in 1D.

The animation below lets you see qualitatively how the typical number of domain walls varies with temperature. If you'd lke to explore more quantitatively, a python code performing a Monte Carlo simulation is available. You will learn about Monte Carlo simulation in the coursework and in later parts of the course.

```
#Monte Carlo simulation of the 1d Ising chain with periodic bounary conditions
import numpy as np
import matplotlib.pyplot as plt
from matplotlib.animation import FuncAnimation
from matplotlib.widgets import Slider

# Number of spins
N = 20

# Initialize spins (+1 or -1)
spins = np.random.choice([-1, 1], size=N)

# Initial temperature
T = 2.0

# Set up figure and axis for the spins
fig, ax = plt.subplots(figsize=(10, 2))
plt.subplots_adjust(bottom=0.25)  # make room for slider
ax.set_xlim(-0.5, N - 0.5)
ax.set_ylim(-1, 1)
ax.axis('off')

# Create text objects for each spin
texts = []
```

```
for i in range(N):
    arrow = '↑' if spins[i] == 1 else '↓'
    t = ax.text(i, 0, arrow, fontsize=24, ha='center', va='center')
    texts.append(t)

def update(frame):
    """Perform Metropolis updates over all spins, then refresh display."""
    global spins, T
    for _ in range(N):
        i = np.random.randint(N)
        left = spins[(i - 1) % N]
        right = spins[(i + 1) % N]
        deltaE = 2 * spins[i] * (left + right)
        # Metropolis criterion ensures configurations appear with the correct Boltzmann proba
        if deltaE < 0 or np.random.rand() < np.exp(-deltaE / T):
            spins[i] *= -1
    # Update arrows on screen
    for idx, t in enumerate(texts):
        t.set_text('↑' if spins[idx] == 1 else '↓')
    return texts

# Create the animation with caching disabled and blit turned off
ani = FuncAnimation(
    fig,
    update,
    interval=200,
    blit=False,
    cache_frame_data=False
)

# Add a temperature slider
ax_T = plt.axes([0.2, 0.1, 0.6, 0.03], facecolor='lightgray')
slider_T = Slider(ax_T, 'Temperature T', 0.1, 5.0, valinit=T)

def on_T_change(val):
    """Callback to update T when the slider changes."""
    global T
    T = val

slider_T.on_changed(on_T_change)

# Show the plot (ani is kept in scope so it won't be deleted)
```

```
plt.show()
```

Temperature T =

2.0

4.2.1 More general 1D spins systems: transfer matrix method

Generally speaking one-dimensional systems lend themselves to a degree of analytic tractability not found in most higher dimensional models. Indeed for the case of a 1-d assembly of N spins each having n discrete energy states, and in the presence of a magnetic field, it is possible to reduce the evaluation of the partition function to the calculation of the eigenvalues of a matrix–the so called transfer matrix.

Let us start by assuming that the assembly has cyclic boundary conditions, then the total energy of configuration $\{s\}$ is

$$\begin{aligned} H(\{s\}) &= -\sum_{i=1}^{N}(Js_is_{i+1} + Hs_i) \\ &= -\sum_{i=1}^{N}(Js_is_{i+1} + H(s_i + s_{i+1})/2) \\ &= \sum_{i=1}^{N} E(s_i, s_{i+1}) \end{aligned}$$

where we have defined $E(s_i, s_{i+1}) = -Js_is_{i+1} - H(s_i + s_{i+1})/2$.

Now the partition function may be written

$$\begin{aligned} Z_N &= \sum_{\{s\}} \exp\left(-\beta H(\{s\})\right) \\ &= \sum_{\{s\}} \exp\left(-\beta[E(s_1, s_2) + E(s_2, s_3) + ...E(s_N, s_1)]\right) \\ &= \sum_{\{s\}} \exp\left(-\beta E(s_1, s_2)\right) \exp\left(-\beta E(s_2, s_3)\right) .... \exp\left(-\beta E(s_N, s_1)\right) \\ &= \sum_{i,j,...,l=1}^{n} V_{ij}V_{jk}...V_{li} \end{aligned}$$

where the $V_{ij} = \exp(-\beta E_{ij})$ are elements of an $n \times n$ matrix $\mathbf{V}$, known as the transfer matrix (i, j, k etc are dummy indices that run over the matrix elements). You should see that the

sum over the product of matrix elements picks up all the terms in the partition function and therefore Equation 4.2 is an alternative way of writing the partition function.

The reason it is useful to transform to a matrix representation is that it transpires that the sum over the product of matrix elements in Equation 4.2 is simply just the trace of $\mathbf{V}^N$ (check this yourself for a short periodic chain), given by the sum of its eigenvalues:-

Proof (non examinable)

Let V be an $n \times n$ matrix, and let $\lambda_1, \ldots, \lambda_n$ denote its eigenvalues.
Every square matrix V can be written as

$$V = QTQ^\dagger,$$

where Q is a unitary matrix ($Q^\dagger Q = I$), and T is upper triangular with the eigenvalues of V on its diagonal:

$$T = \begin{pmatrix} \lambda_1 & * & \cdots & * \\ 0 & \lambda_2 & \cdots & * \\ \vdots & & \ddots & \vdots \\ 0 & \cdots & 0 & \lambda_n \end{pmatrix}.$$

Raising both sides to the Nth power gives

$$V^N = (QTQ^\dagger)^N = Q\,T^N\,Q^\dagger.$$

The trace (ie. the sum of diagonal elements) is invariant under similarity transformations:

$$\mathrm{Tr}(V^N) = \mathrm{Tr}(T^N).$$

Since T is upper triangular, so is T^N. The diagonal elements of T^N are simply the Nth powers of the diagonal elements of T, i.e.

$$(T^N)_{ii} = (T_{ii})^N = \lambda_i^N.$$

Therefore,

$$\mathrm{Tr}(T^N) = \sum_{i=1}^{n} (T^N)_{ii} = \sum_{i=1}^{n} \lambda_i^N.$$

$$Z_N = \lambda_1^N + \lambda_2^N + \ldots \lambda_m^N$$

For very large N, this expression simplifies further because the largest eigenvalue λ_1 dominates the behaviour since $(\lambda_2/\lambda_1)^N$ vanishes as $N \to \infty$. Consequently in the thermodynamic limit one may put $Z_N = \lambda_1^N$ and the problem reduces to identifying the largest eigenvalue of the transfer matrix.

Specializing to the case of the simple Ising model in the presence of an applied field H, the transfer matrix takes the form

$$\mathbf{V}(H) = \begin{pmatrix} e^{\beta(J+H)} & e^{-\beta J} \\ e^{-\beta J} & e^{\beta(J-H)} \end{pmatrix}$$

This matrix has two eigenvalues which can be readily calculated in the usual fashion as the roots of the characteristic polynomial $|\mathbf{V} - \lambda\mathbf{I}|$. They are

$$\lambda_{\pm} = e^{\beta J}\cosh(\beta H) \pm \sqrt{e^{2\beta J}\sinh^2 \beta H + e^{-2\beta J}}.$$

Hence the free energy per spin $f = -k_B T \ln \lambda_+$ is

$$f = -k_B T \ln \left[e^{\beta J}\cosh(\beta H) + \sqrt{e^{2\beta J}\sinh^2 \beta H + e^{-2\beta J}} \right].$$

The Ising model in 2D can also be solved exactly, as was done by Lars Onsager in 1940. The solution is extremely complicated and is regarded as one of the pinnacles of statistical mechanics. In 3D no exact solution is known.

More about the scientists mentioned in this chapter:

Lars Onsager

Ernst Ising

5 Mean field theory and perturbation schemes

Of the wide variety of models of interest to the critical point theorist, the majority have shown themselves intractable to direct analytic (pen and paper) assault. In a very limited number of instances models have been solved exactly, yielding the phase coexistence parameters, critical exponents and the critical temperature. The 2-d spin-$\frac{1}{2}$ Ising model is certainly the most celebrated such example, its principal critical exponents are found to be $\beta = \frac{1}{8}, \nu = 1, \gamma = \frac{7}{4}$. Its critical temperature is $-2J/\ln(\sqrt{2}-1) \approx 2.269J$. Unfortunately such solutions rarely afford deep insight to the general framework of criticality although they do act as an invaluable test-bed for new and existing theories.

The inability to solve many models exactly often means that one must resort to approximations. One such approximation scheme is mean field theory.

5.1 Mean field solution of the Ising model

Let us look for a mean field expression for the free energy of the Ising model whose Hamiltonian is given in Equation 4.1 . Write

$$s_i = \langle s_i \rangle + (s_i - \langle s_i \rangle) = m + (s_i - m) = m + \delta s_i$$

Then

$$\begin{aligned} H_I =& -J \sum_{<i,j>} [m + (s_i - m)][m + (s_j - m)] - H \sum_i s_i \\ =& -J \sum_{<i,j>} [m^2 + m(s_i - m) + m(s_j - m) + \delta s_i \delta s_j] - H \sum_i s_i \\ =& -J \sum_i (qms_i - qm^2/2) - H \sum_i s_i - J \sum_{<i,j>} \delta s_i \delta s_j \end{aligned}$$

where in the last line we transformed from a sum over bonds to a sum over sites. Doing so makes use of the fact that when for each site i we perform the sum $\sum_{<i,j>}$ over bonds of a quantity which is independent of s_j, then the result is just the number of bonds per site times that quantity. Since the number of bonds on a lattice of N sites of coordination q is $Nq/2$ (because each bond is shared between two sites), there are therefore $q/2$ bonds per site.

Now the mean field approximation is to ignore the last term in the last line of Equation 5.1 giving the configurational energy as

$$H_{mf} = -\sum_i H_{mf} s_i + NqJm^2/2$$

with $H_{mf} \equiv qJm + H$ the "mean field" seen by spin s_i. As all the spins are decoupled (independent) in this approximation we can write down the partition function, which follows by taking the partition function for a single spin (by summing the Boltzmann factor for $s_i = \pm 1$) and raising to the power N to find

$$Z = e^{-\beta qJm^2 N/2} [2\cosh(\beta(qJm + H))]^N$$

The free energy follows as

$$F(m) = NJqm^2/2 - Nk_B T \ln[2\cosh(\beta(qJm + H)] \,.$$

and the magnetisation as

$$m = -\frac{1}{N}\frac{\partial F}{\partial H} = \tanh(\beta(qJm + H)),$$

where the first term drops out because we treat m as an independent variable when differentiating w.r.t. H.

This is a self consistent equation because m appears on both the left and the right hand sides. To find $m(H, T)$, we must numerically solve this last equation-self consistently. You will meet such an equation again later when you learn about mean field theories for liquid crystals.

> **Why self-consistent?**
>
> In mean-field theory, the many-body interaction is replaced by an effective one-body problem in which each degree of freedom experiences an average field generated by all the others. The quantity that characterises the ordered phase—the order parameter—is precisely this average. Because the effective (mean-field) Hamiltonian is constructed using a *presumed* value of that average, internal consistency requires that the order parameter obtained by solving the effective problem *match* the value assumed to define it. Enforcing this equality yields a self-consistency condition for the order parameter. In practice: choose the effective field determined by the putative order parameter, compute the corresponding thermal average, and require that the two coincide.

Note that we can obtain m in a different way. Consider some arbitary spin, s_i say. Then this spin has an energy $H_{mf}(s_i)$. Considering this energy for both cases $s_i = \pm 1$ and the probability $p(s_i) = e^{-\beta H_{mf}(s_i)}/Z$ of each, we have that

$$\langle s_i \rangle = \sum_{s_i=\pm 1} s_i p(s_i)$$

but for consistancy, $\langle s_i \rangle = m$. Thus

$$\begin{aligned} m &= \sum_{s_i=\pm 1} s_i p(s_i) \\ &= \frac{e^{\beta(qJm+H)} - e^{-\beta(qJm+H)}}{e^{\beta(qJm+H)} + e^{-\beta(qJm+H)}} \\ &= \tanh(\beta(qJm + H)) \end{aligned}$$

as before.

5.2 Spontaneous symmetry breaking

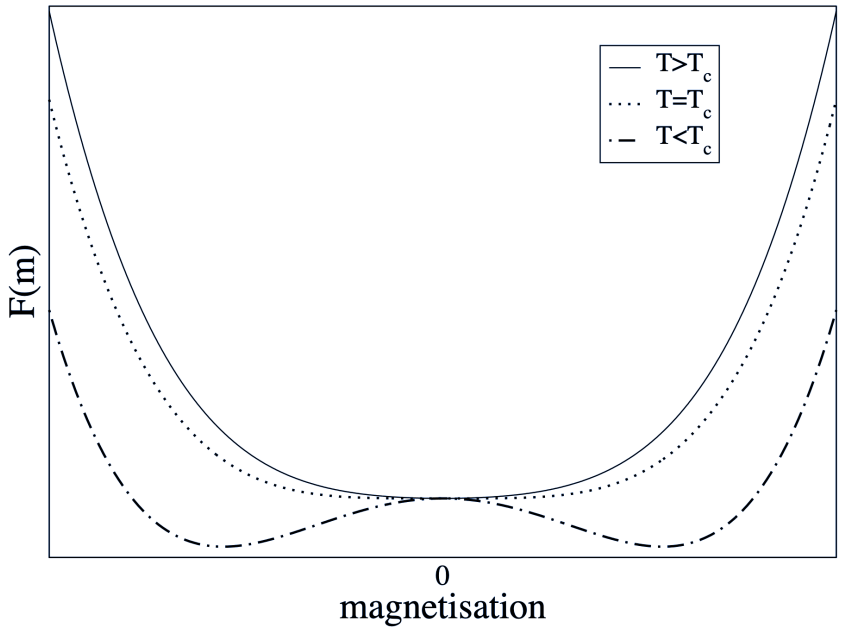


Figure 5.1: Schematic of the form of the free energy for a critical, subcritical and supercritical temperature

This mean field analysis reveals what is happening in the Ising model near the critical temperature T_c. Figure 5.1 shows sketches for $\beta F(m)/N$ as a function of temperature, where for f simplicity we restrict attention to $H = 0$. In this case $F(m)$ is symmetric in m, Moreover, at high T, the entropy dominates and there is a single minimum in $F(m)$ at $m = 0$. As T is

lowered, there comes a point ($T = T_c = qJ/k_B$) where the curvature of $F(m)$ at the origin changes sign; precisely at this point

$$\frac{\partial^2 F}{\partial m^2} = 0.$$

At lower temperature, there are instead two minima at nonzero $m = \pm m^\star$, where the *equilibrium magnetisation* $m^\star$ is the positive root (calculated explicitly below) of

$$m^\star = \tanh(\beta J q m^\star) = \tanh(\frac{m^\star T_c}{T})$$

The point $m = 0$ which remains a root of this equation, is clearly an unstable point for $T < T_c$ (since F has a maximum there).

This is an example of spontaneous symmetry breaking. In the absence of an external field, the Hamiltonian (and therefore the free energy) is symmetric under $m \to -m$. Accordingly, one might expect the actual state of the system to also show this symmetry. This is true at high temperature, but spontaneously breaks down at low ones. Instead there are a pair of ferromagnetic states (spins mostly up, or spins mostly down) which – by symmetry– have the same free energy, lower than the unmagnetized state.

5.3 Phase diagram

The resulting zero-field magnetisation curve $m(T, H = 0)$ looks like Figure 5.2.

This shows the sudden change of behaviour at T_c (phase transition). For $T < T_c$ it is arbitrary which of the two roots $\pm m^\star$ is chosen; typically it will be different in different parts of the sample (giving macroscopic "magnetic domains"). But this behaviour with temperature is *qualitatively modified* by the presence of a field H, however small. In that case, there is always a slight magnetization, even far above T_c and the curves becomes smoothed out, as shown. There is no doubt which root will be chosen, and no sudden change of the behaviour (no phase transition). Spontaneous symmetry breaking does not occur, because the symmetry is already broken by H. (The curve $F(m)$ is lopsided, rather than symmetrical about $m = 0$.)

On the other hand, if we sit below T_c in a positive field (say) and gradually reduce H through zero so that it becomes negative, there is a *very* sudden change of behaviour at $h = 0$: the equilibrium state jumps discontinuously from $m = m^\star$ to $m = -m^\star$.

This is called a first order phase transition as opposed to the "second order" or continuous transition that occurs at T_c in zero field. The definitions are:

First order transition: magnetisation (or similar order parameter) depends discontinuously on a field variable (such as h or T).

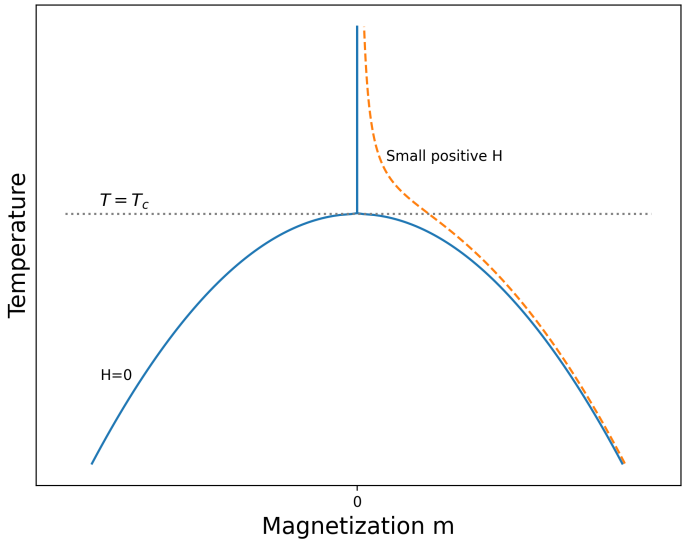


Figure 5.2: Phase diagram of a simple magnet in the m-T plane.

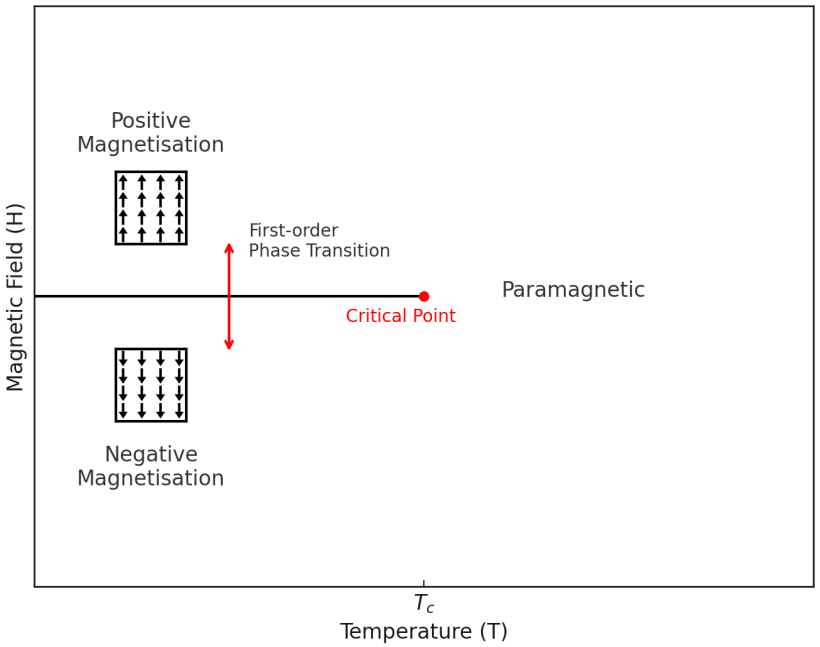


Figure 5.3: Phase diagram of a simple magnet in the H-T plane.

Continuous transition (criticality): Change of functional form, but no discontinuity in m; typically, however, $(\partial m/\partial T)_h$ (or similar) is either discontinuous, or diverges with an integrable singularity.

In this terminology, we can say that the phase diagram of the magnet in the H, T plane shows a line of first order phase transitions, terminating at a continuous transition, which is the critical point.

> Aside on Quantum Criticality
>
> In some magnetic systems such as $CePd_2Si_2$, one can, by applying pressure or altering the chemical composition, depress the critical temperature all the way to abolute zero! This may seem counterintuitive, after all at $T = 0$ one should expect perfect ordering, not the large fluctuations that accompany criticality. It turns out that the source of the fluctuations that drive the system critical is zero point motion associated with the Heisenberg uncertainty principle. Quantum criticality is a matter of ongoing active research, and open questions concern the nature of the phase diagrams and the relationship to superconductivity. Although the subject goes beyond the scope of this course, there is an accessible article here if you want to learn more.

5.4 A closer look: critical exponents

Let us now see how we can calculate critical exponents within the mean field approximation.

5.4.1 Zero H solution and the order parameter exponent

In zero field

$$m = \tanh(\frac{mT_c}{T})$$

where $T_c = qJ/k_B$ is the critical temperature at which m first goes to zero.

We look for a solution where m is small ($\ll 1$). Expanding the tanh function and replacing $\beta = (k_B T)^{-1}$ yields

$$m = \frac{mT_c}{T} - \frac{1}{3}\left(\frac{mT_c}{T}\right)^3 + O(m^5)\,.$$

Then $m = 0$ is one solution. The other solution is given by

$$m^2 = 3\left(\frac{T}{T_c}\right)^3\left(\frac{T_c}{T}-1\right)$$

Now, considering temperatures close to T_c to guarantee small m, and employing the reduced temperature $t = (T - T_c)/T_c$, one finds

$$m^2 \simeq -3t$$

Hence

$$\begin{aligned} m &= 0 \quad \text{for } T > T_c \text{ since otherwise } m \text{ imaginary} \\ m &= \pm\sqrt{-3t} \quad \text{for } T < T_c \quad \text{real} \end{aligned} \tag{5.1}$$

This result implies that (within the mean field approximation) the critical exponent $\beta = 1/2$.

5.4.2 Finite (but small) field solution: the susceptibility exponent

In a finite, but small field we can expand Equation 5.1 thus:

$$m = \frac{mT_c}{T} - \frac{1}{3}\left(\frac{mT_c}{T}\right)^3 + \frac{H}{kT}$$

Consider now the isothermal susceptibility

$$\begin{aligned} \chi &\equiv \left(\frac{\partial m}{\partial H}\right)_T \\ &= \frac{T_c}{T}\chi - \left(\frac{T_c}{T}\right)^3 \chi m^2 + \frac{1}{k_B T} \end{aligned}$$

Then

$$\chi\left[1 - \frac{T_c}{T} + \left(\frac{T_c}{T}\right)^3 m^2\right] = \frac{1}{k_B T}$$

Hence near T_c

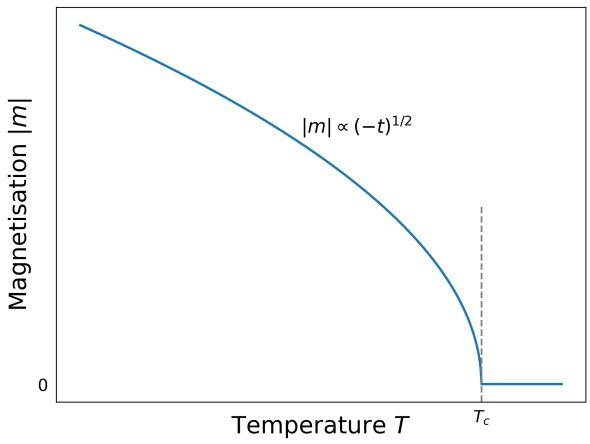
$$\chi = \frac{1}{k_B T_c}\left(\frac{1}{t + m^2}\right)$$

Then using the results of Equation 5.1

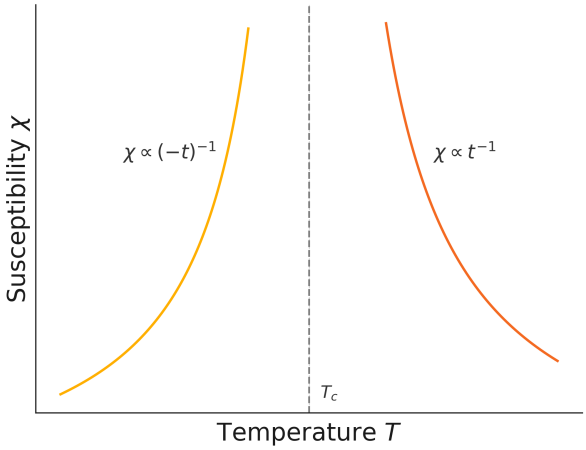
$$\chi = (k_B T_c t)^{-1} \text{ for } \quad T > T_c$$
$$\chi = (-2k_B T_c t)^{-1} \text{ for } \quad T \leq T_c$$

where one has to take the non-zero value for m below T_c to ensure +ve χ, i.e. thermodynamic stability. This result implies that (within the mean field approximation) the critical exponent $\gamma = 1$.

The schematic behaviour of the Ising order parameter and susceptibility are shown in Figure 5.5 (a) and (b) respectively.



(a) Mean field behaviour of the Ising magnetisation (schematic)



(b) Mean field behaviour of the Ising susceptibility (schematic)

5.5 Landau theory

Landau theory is a slightly more general type of mean field theory than that discussed in the previous subsection because it is not based on a particular microscopic model. Its starting point is the Helmholtz free energy, which Landau asserted can be written in terms of power series expansion of the order parameter ϕ:

$$F(\phi) = \sum_{i=0}^{\infty} a_i \phi^i$$

The equilibrium value of ρ is that which minimises the Landau free energy.

A note on order parameters

We have already seen examples of these in earlier sections, e.g., for the liquid-gas transition this was

$$\rho_{liq} - \rho_{gas}: \quad \text{difference in density of two coexisting phases,}$$

while for the Ising magnet it is the magnetisation m. Both quantities vanish at the critical point. These are examples of *scalar* order parameters – a single number is required to represent the degree of order ($n = 1$).
In the absence of a symmetry-breaking field, the Landau free-energy density f_L must have symmetry $f_L(-\phi) = f_L(\phi)$ (Ising case).
For some other systems, n component vectors are required in order to represent the order:

$$\phi = (\phi_1, \phi_2, \dots, \phi_n)$$

Then $f_L(\phi)$ should be symmetric under $O(n)$ rotations in n-component ϕ-space.
The table below lists examples of order parameters for various physical systems.

Physical System	Order Parameter φ	Symmetry Group
Uniaxial (Ising) ferromagnet	Magnetisation per spin, m	$O(1)$
Fluid (liquid-gas)	Density difference, $\rho - \rho_c$	$O(1)$
Liquid mixtures	Concentration difference, $c - c_c$	$O(1)$
Binary (AB) alloy (e.g., β-brass)	Concentration of one of the species, c	$O(1)$
Isotropic (vector) ferromagnet	n-component magnetisation, $\mathbf{m} = (m_1, m_2, \dots, m_n)$	$O(n)$
	$n = 2$: xy model	$O(2)$
	$n = 3$: Heisenberg model	$O(3)$
Superfluid He^4	Macroscopic condensate wavefunction, Ψ	$O(2)$
Superconductor (s-wave)	Macroscopic condensate wavefunction, Ψ	$O(2)$
Nematic liquid crystal	Orientational order, $\langle P_2(\cos\theta)\rangle$	
Smectic A liquid crystal	1-dimensional periodic density	
Crystal	3-dimensional periodic density	

Notes:

- In **superfluid** ^4He the order parameter is

$$\Psi = |\Psi| e^{i\theta},$$

the *complex wavefunction* of the macroscopic condensate. Both the amplitude $|\Psi|$ and phase θ must be specified, so this corresponds to $n = 2$.
Superconductors also correspond to $n = 2$.

- In a **nematic** liquid crystal, the *orientational* order parameter is

$$\langle P_2(\cos\theta)\rangle \equiv \frac{1}{2}\langle 3\cos^2\theta - 1\rangle,$$

where θ is the angle a molecule makes with the average direction of the long axes of the molecules (known as the *director* $\hat{n}$). Rotational symmetry is broken. For the case of an n component vector, the free energy should be a function of:

$$\phi^2 \equiv |\phi|^2 = \phi_1^2 + \phi_2^2 + \cdots + \phi_n^2 = \sum_{i=1}^{n} \phi_i^2$$

in the absence of a symmetry breaking field. Rotational symmetry is incorporated into the theory.



(a) Schematic of the isotropic liquid phase of a system of elongated molcules.



(b) Schematic of the nematic liquid phase of a system elongated molcules. This phase has uniaxial ordering.

Figure 5.5: Isotropic and uniaxially ordered (nematic) phases of liquid crystal molecules.

To exemplify the approach, let us specialise to the case of a ferromagnet where $\phi = m$, the magnetisation and write the Landau free energy as

$$F(m) = F_0 + a_2 m^2 + a_4 m^4 \tag{5.2}$$

Here only the terms compatible with the order parameter symmetry are included in the expansion and we truncate the series at the 4th power because this is all that is necessary to yield the essential phenomenology. On symmetry grounds, the free energy of a ferromagnet should be invariant under a reversal of the sign of the magnetisation. Terms linear and cubic in m are not invariant under $m \to -m$, and so do not feature.

One can understand how the Landau free energy can give rise to a critical point and coexistence values of the magnetisation, by plotting $F(m)$ for various values of a_2 with a_4 assumed positive (which ensures that the magnetisation remains bounded). This is shown in the following movie:

Movies/landau_free_energy_evolution.mp4

The situation is qualitatively similar to that discussed in Section 5.2. Thermodynamics tells us that the system adopts the state of lowest free energy. From the movie, we see that for $a_2 > 0$, the system will have $m = 0$, i.e. will be in the disordered (or paramagnetic) phase. For $a_2 < 0$, the minimum in the free energy occurs at a finite value of m, indicating that the ordered (ferromagnetic) phase is the stable one. In fact, the physical (up-down) spin symmetry built into F indicates that there are two equivalent stable states at $m = \pm m^\star$. $a_2 = 0$ corresponds to the critical point which marks the border between the ordered and disordered phases. Note that it is an inflexion point, so has $\frac{d^2F}{dm^2} = 0$.

Clearly a_2 controls the deviation from the critical temperature, and accordingly we may write

$$a_2 = \tilde{a_2} t$$

where t is the reduced temperature. Thus we see that the trajectory of the minima as a function of $a_2 < 0$ in the above movie effective traces out the coexistence curve in the $m - T$ plane.

We can now attempt to calculate critical exponents. Restricting ourselves first to the magnetisation exponent β defined by $m = t^\beta$, we first find the equilibrium magnetisation, corresponding to the minimum of the Landau free energy:

$$\frac{dF}{dm} = 2\tilde{a_2} t m + 4 a_4 m^3 = 0 \tag{5.3}$$

which implies

$$m \propto (-t)^{1/2},$$

so $\beta = 1/2$, which is again a mean field result.

Likewise we can calculate the effect of a small field H if we sit at the critical temperature T_c. Since $a_2 = 0$, we have

$$F(m) = F_0 + a_4 m^4 - Hm$$

$$\frac{\partial F}{\partial m} = 0 \Rightarrow m(H, T_c) = \left(\frac{H}{4a_4}\right)^{1/3}$$

or

$$H \sim m^\delta \qquad \delta = 3$$

which defines a second critical exponent.

Note that at the critical point, a small applied field causes a very big increase in magnetisation; formally, $(\partial m/\partial H)_T$ is infinite at $T = T_c$.

A third critical exponent can be defined from the magnetic susceptibility at zero field

$$\chi = \left(\frac{\partial m}{\partial H}\right)_{T,V} \sim |T - T_c|^{-\gamma}$$

Exercise: Show that the Landau expansion predicts $\gamma = 1$.

Finally we define a fourth critical exponent via the variation of the heat capacity (per site or per unit volume) C_H, in fixed external field $H = 0$:

$$C_H \sim |T - T_c|^{-\alpha}$$

By convention, α is defined to be positive for systems where there is a *divergence* of the heat capacity at the critical point (very often the case). The heat capacity can be calculated from

$$C_H = -T\frac{\partial^2 F}{\partial T^2}$$

From the minimization over m Equation 5.3 one finds (*exercise*: check this)

$$\begin{aligned} F &= 0 \quad T > T_c \\ F &= -a_2^2/4a_4 \quad T < T_c \end{aligned}$$

Using the fact that a_2 varies linearly with T, we have

$$C_H = 0 \quad T \to T_c^+$$
$$C_H = \frac{T\tilde{a}_2^2}{2a_4} \quad T \to T_c^- \,,$$

which is actually a step discontinuity in specific heat. Since for positive α the heat capacity is divergent, and for negative α it is continuous, this behaviour formally corresponds to $\alpha = 0$

5.6 Shortcomings of mean field theory

While mean field theories provide a useful route to understanding qualitatively the phenomenology of phase transitions, in real ferromagnets, as well as in more sophisticated theories, the critical exponents are not the simple fraction and integers found here. This failure of mean field theory to predict the correct exponents is of course traceable to their neglect of correlations. In later sections we shall start to take the first steps to including the effects of long range correlations.

Table 5.2: Comparison of true Ising critical exponents with their mean field theory predictions in a number of dimensions.

	Mean Field	$d = 1$	$d = 2$	$d = 3$
Critical temperature $k_B T/qJ$	1	0	0.5673	0.754
Order parameter exponent β	$\frac{1}{2}$	-	$\frac{1}{8}$	0.325 ± 0.001
Susceptibility exponent γ	1	∞	$\frac{7}{4}$	1.24 ± 0.001
Correlation length exponent ν	$\frac{1}{2}$	∞	1	0.63 ± 0.001

More about the scientists mentioned in this chapter:

Lev D. Landau

6 The Static Scaling Hypothesis

Historically, the first step towards properly elucidating near-critical behaviour was taken with the static scaling hypothesis. This is essentially a plausible conjecture concerning the origin of power law behaviour which appears to be consistent with observed phenomena. According to the hypothesis, the basis for power law behaviour (and associated scale invariance or "scaling") in near-critical systems is expressed in the claim that: in the neighbourhood of a critical point, the basic thermodynamic functions (most notably the free energy) are *generalized homogeneous functions* of their variables. For such functions one can always deduce a scaling law such that by an appropriate change of scale, the dependence on two variables (e.g. the temperature and applied field) can be reduced to dependence on one new variable. This claim may be warranted by the following general argument.

A function of two variables $g(u, v)$ is called a generalized homogeneous function if it has the property

$$g(\lambda^a u, \lambda^b v) = \lambda g(u, v)$$

for all λ, where the parameters a and b (known as scaling parameters) are constants. An example of such a function is $g(u, v) = u^3 + v^2$ with $a = 1/3, b = 1/2$.

Now, the arbitrary scale factor λ can be redefined without loss of generality as $\lambda^a = u^{-1}$ giving

$$g(u, v) = u^{1/a} g(1, \frac{v}{u^{b/a}})$$

A corresponding relation is obtained by choosing the rescaling to be $\lambda^b = v^{-1}$.

$$g(u, v) = v^{1/b} g(\frac{u}{v^{a/b}}, 1)$$

This equation demonstrates that $g(u, v)$ indeed satisfies a simple power law in *one* variable, subject to the constraint that $u/v^{a/b}$ is a constant. It should be stressed, however, that such a scaling relation specifies neither the function g nor the parameters a and b.

Now, the static scaling hypothesis asserts that in the critical region, the free energy F is a generalized homogeneous function of the (reduced) thermodynamic fields $t = (T - T_c)/T_c$ and

$h = (H - H_c)$. Remaining with the example ferromagnet, the following scaling assumption can then be made:

$$F(\lambda^a t, \lambda^b h) = \lambda F(t, h) \, .$$

Without loss of generality, we can set $\lambda^a = t^{-1}$, implying $\lambda = t^{-1/a}$ and $\lambda^b = t^{-b/a}$.

Then

$$F(t, h) = t^{1/a} F(1, t^{-b/a} h)$$

where our choice of λ ensures that F on the rhs is now a function of a single variable $t^{-b/a}h$.

Now, as stated in Chapter 2, the free energy provides the route to all thermodynamic functions of interest. An expression for the magnetisation can be obtained simply by taking the field derivative of F (cf. Figure 2.1)

$$m(t, h) = (-t)^{(1-b)/a} m(1, t^{-b/a} h) \tag{6.1}$$

In zero applied field $h = 0$, this reduces to

$$m(t, 0) = (-t)^{(1-b)/a} m(1, 0)$$

where the r.h.s. is a power law in t. Equation 3.4 then allows identification of the exponent β in terms of the scaling parameters a and b.

$$\beta = \frac{1 - b}{a}$$

By taking further appropriate derivatives of the free energy, other relations between scaling parameters and critical exponents may be deduced. Such calculations (*Exercise: try to derive them*) yield the results $\delta = b/(1 - b)$,$\gamma = (2b - 1)/a$, and $\alpha = (2a - 1)/a$. Relationships between the critical exponents themselves can be obtained trivially by eliminating the scaling parameters from these equations. The principal results (known as "scaling laws") are:-

$$\alpha + \beta(\delta + 1) = 2$$
$$\alpha + 2\beta + \gamma = 2$$

Thus, provided all critical exponents can be expressed in terms of the scaling parameters a and b, then only two critical exponents need be specified, for all others to be deduced. Of course these scaling laws are also expected to hold for the appropriate thermodynamic functions of analogous systems such as the liquid-gas critical point.

6.1 Experimental Verification of Scaling

The validity of the scaling hypothesis finds startling verification in experiment. To facilitate contact with experimental data for real systems, consider again Equation 6.1. Eliminating the scaling parameters a and b in favour of the exponents β and δ gives

$$\frac{m(t,h)}{t^{\beta}} = m(1, \frac{h}{t^{\beta\delta}})$$

where the RHS of this last equation can be regarded as a function of the single scaled variable $\tilde{H} \equiv t^{-\beta\delta}h(t,M)$.

For some particular magnetic system, one can perform an experiment in which one measures m vs h for various fixed temperatures. This allows one to draw a set of isotherms, i.e. $m-h$ curves of constant t. These can be used to demonstrate scaling by plotting the data against the scaling variables $M = t^{-\beta}m(t,h)$ and $\tilde{H} = t^{-\beta\delta}h(t,M)$. Under this scale transformation, it is found that all isotherms (for t close to zero) coincide to within experimental error. Reassuringly, similar results are found using the scaled equation of state of simple fluid systems such as He^3 or Xe.

In summary, the static scaling hypothesis is remarkably successful in providing a foundation for the observation of power laws and scaling phenomena. However, it furnishes little or no guidance regarding the role of co-operative phenomena at the critical point. In particular it provides no means for calculating the values of the critical exponents appropriate to given model systems.

6.2 Computer simulation

In seeking to employ simulation to obtain estimates of bulk critical point properties (such as the location of a critical point and the values of its associated exponents), one is immediately confronted with a difficulty. The problem is that simulations are necessarily restricted to dealing with systems of finite-size and cannot therefore accommodate the truly long ranged fluctuations that characterize the near-critical regime. As a consequence, the critical singularities in C_v, order parameter, etc. appear rounded and shifted in a simulation study. Figure 6.2 shows a schematic example for the susceptibility of a magnet.

Thus the position of the peak in a response function (such as C_v) measured for a finite-sized system does not provide an accurate estimate of the critical temperature. Although the degree of rounding and shifting reduces with system size, it is often the case, that computational constraints prevent access to the largest system sizes which would provide accurate estimates of critical parameters. To help deal with this difficulty, finite-size scaling (FSS) methods have been developed to allow extraction of bulk critical properties from simulations of finite size. FSS will be discussed in section 7.

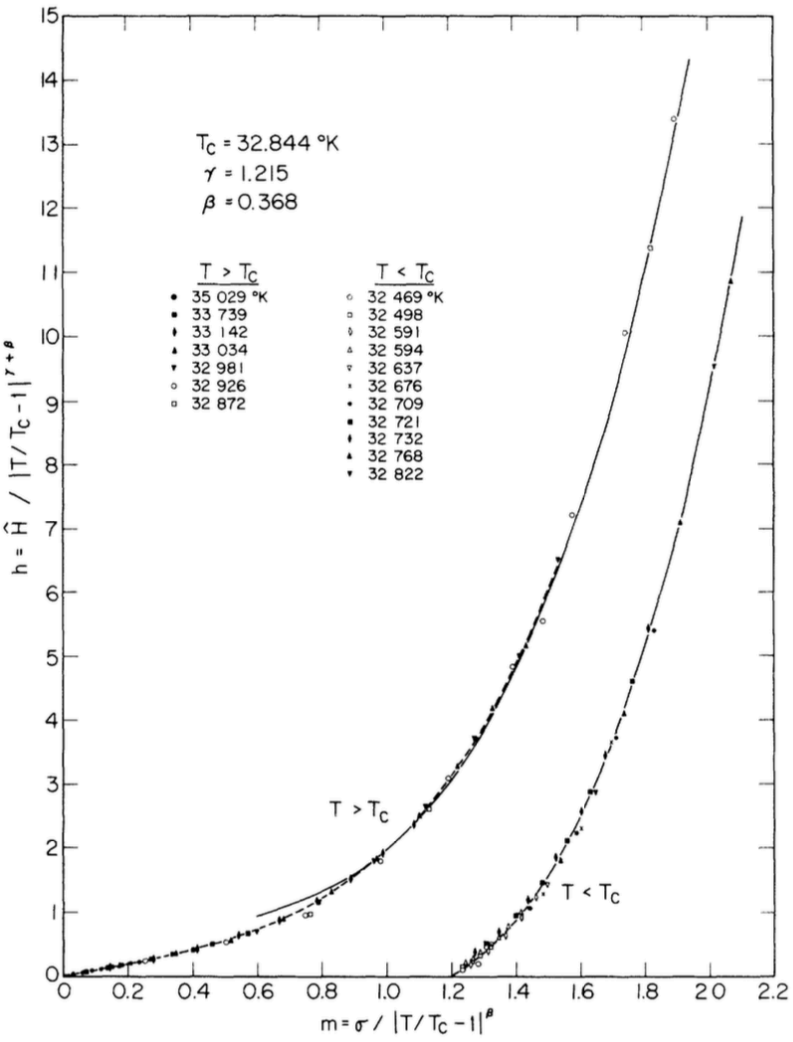


Figure 6.1: Magnetisation of $CrBr_3$ in the critical region plotted in scaled form (see text). From Ho and Lister (1969).

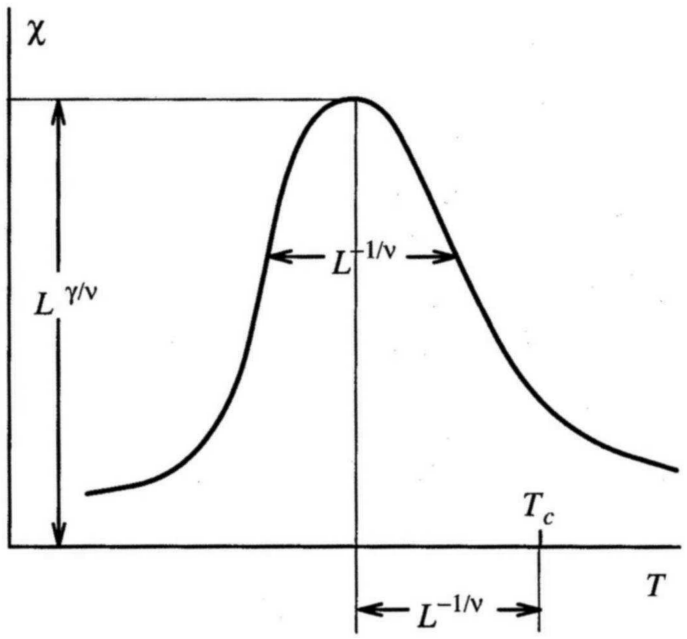


Figure 6.2: Schematic of the near-critical temperature dependence of the magnet susceptibility in a finite-sized system.

7 Universality and the Renormalisation Group Theory of Critical Phenomena

Owing the the absence of a wholly appropriate textbook for the material covered in this section, I have supplied more detailed notes than used in other parts of the unit.

The critical region is characterised by correlated microstructure on *all* length-scales up to and including the correlation length.

Such a profusion of degrees of freedom can only be accurately characterized by a very large number of variables. Mean field theories and approximation schemes fail in the critical region because they at best incorporate interactions among only a few spins, while neglecting correlations over larger distances. Similarly, the scaling hypothesis fails to provide more than a qualitative insight into the nature of criticality because it focuses on only one length-scale, namely the correlation length itself. Evidently a fuller understanding of the critical region may only be attained by taking account of the existence of structure on all length-scales. Such a scheme is provided by the renormalisation group method, which stands today as the cornerstone of the modern theory of critical phenomena.

7.1 The critical point: A many length scale problem

A near critical system can be characterized by three important length scales, namely

1. The correlation length, ξ, ie the size of correlated microstructure.
2. Minimum length scale $L_{\min}$, i.e. the smallest length in the microscopics of the problem, e.g. lattice spacing of a magnet or the particle size in a fluid.
3. Macroscopic size $L_{\max}$ eg. size of the system.

The authentic critical region is defined by a window condition:

$$L_{\max} \gg \xi \gg L_{\min}$$

The physics of this regime is hard to tackle by analytic theory because it is characterized by configurational structure on all scales between $L_{\min}$ and ξ (in fact it turns out that the near critical configurational patterns are *fractal*-like, cf. Figure 4.1b. Moreover different length

scales are correlated with one another, giving rise to a profusion of coupled variables in any theoretical description. The window regime is also not easily accessed by computer simulation because it entails studying very large system sizes $L_{\max}$, often requiring considerable computing resources.

A nice illustration of critical point scale invariance in the Ising model can be viewed here.

7.2 Methodology of the RG

The central idea of the renormalisation group (RG) method is a stepwise elimination of the degrees of freedom of the system on successively larger length-scales. To achieve this one introduces a fourth length scale L. In contrast to the other three, which characterize the system itself, L characterises the *description* of the system. It may be thought of as typifying the size of the smallest resolvable detail in a description of the system's microstructure.

Consider the Ising model arrangements displayed in Figure 4.1. These pictures contain *all* the details of each configuration shown: the resolution length L in this case has its smallest possible value, coinciding with the lattice spacing i.e. $L = L_{\min}$. In the present context, the most detailed description is not the most useful: the essential signals with which we are concerned are hidden in a noise of relevant detail. A clue to eliminating this noise lies in the nature of the correlation length, i.e. the size of the largest droplets. The explicit form of the small scale microstructure is irrelevant to the behaviour of ξ. The small scale microstructure is the noise. To eliminate it, we simply select a larger value of the resolution length (or 'coarse-graining' length) L.

There are many ways of implementing this coarse-graining procedure. We adopt a simple strategy in which we divide our sample into blocks of side L, each of which contains L^d sites, with d the space dimensions . The centres of the blocks define a lattice of points indexed by $I = 1, 2, ..., N/L^d$. We associate with each block lattice point centre, I, a coarse-grained or block variable $S(L)$ defined as the spatial average of the local variables it contains:

$$S(L) = L^{-d} \sum_{i}^{I} s_i \tag{7.1}$$

where the sum extends over the L^d sites in the block I. The set of coarse grained coordinates $\{S(L)\}$ are the basic ingredients of a picture of the system having spatial resolution of order L.

The coarse graining operation is easily implemented on a computer. In so doing one is faced with the fact that while the underlying Ising spins can only take two possible values, the block variables $S(L)$ have $L^d + 1$ possible values. Accordingly in displaying the consequences of the blocking procedure, we need a more elaborate colour convention than that used in Figure 4.1.

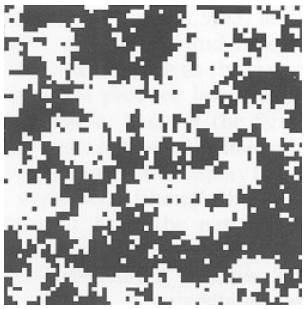
We will associate with each block a shade of grey drawn from a spectrum ranging from black to white.

The results of coarse-graining configurations typical of three different temperatures are shown in Figure 7.1 and Figure 7.2. Two auxiliary operations are implicit in these results. The first operation is a *length scaling*: the lattice spacing on each blocked lattice has been scaled to the same size as that of the original lattice, making possible the display of correspondingly larger portions of the physical system. The second operation is a *variable scaling*: loosely speaking, we have adjusted the scale ('contrast') of the block variable so as to match the spectrum of block variable values to the spectrum of shades at our disposal.

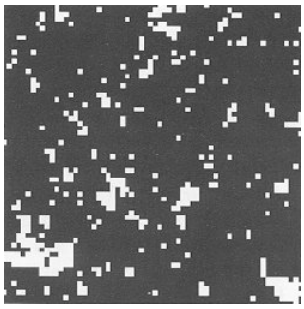
Consider first a system marginally above its critical point at a temperature T chosen so that the correlation length ξ is approximately 6 lattice spacing units. A typical arrangement (without coarse-graining) is shown in Figure 7.1(ai). The succeeding panels, (aii) and (aiii), show the result of coarse-graining with block sizes $L = 4$ and $L = 8$, respectively. A clear trend is apparent. The coarse-graining *amplifies* the consequences of the small deviation of T from T_c. As L is increased, the ratio of the size of the largest configurational features (ξ) to the size of the smallest (L) is reduced. The ratio ξ/L provides a natural measure of how 'critical' is a configuration. Thus the coarse-graining operation generates a representation of the system that is effectively less critical the larger the coarse-graining length. The limit point of this trend is the effectively fully disordered arrangement shown in Figure 7.1(aiii) and in an alternative form in Figure 7.1(aiv), which shows the limiting distribution of the coarse grained variables, averaged over many realizations of the underlying configurations: the distribution is a Gaussian which is narrow (even more so the larger the L value) and centred on zero. This limit is easily understood. When the system is viewed on a scaled L larger than ξ, the correlated microstructure is no longer explicitly apparent; each coarse-grained variable is essentially independent of the others.

A similar trend is apparent below the critical point. Figure 7.1(bi) show a typical arrangement at a temperature $T < T_c$ such that again ξ is approximately 6 lattice spacings. Coarse-graining with $L = 4$ and $L = 8$ again generates representations which are effectively less critical as shown in panels (bii) and (biii)). This time the coarse-graining smoothes out the microstructure which makes the order incomplete. The limit point of this procedure is a homogeneously ordered arrangement in which the block variables have a random (Gaussian) distribution centred on the order parameter (Figure 7.1(biv)).

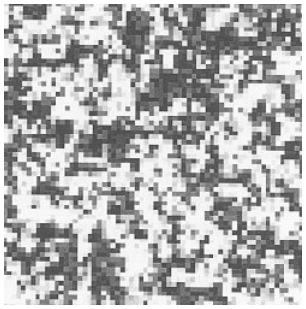
Consider now the situation *at* the critical point. Figure 7.2(ai) shows a typical arrangement; panels (aii) and (aiii) show the results of coarse-graining with $L = 4$ and $L = 8$ respectively. Since the ξ is as large as the system itself the coarse graining does not produce less critical representations of the physical system: each of the figures displays structure over *all* length scales between the lower limit set by L and the upper limit set by the size of the display itself. A limiting trend is nevertheless apparent. Although the $L = 4$ pattern is qualitatively quite different from the pattern of the local variables, the $L = 4$ and $L = 8$ patterns display qualitatively similar features. These similarities are more profound than is immediately apparent. A statistical analysis of the spectrum of $L = 4$ configurations (generated as the local



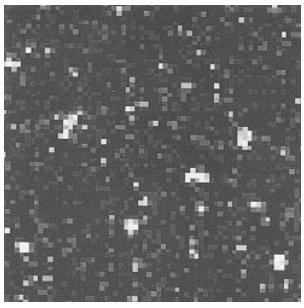
(a) (ai)



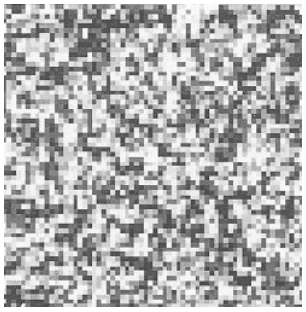
(b) (bi)



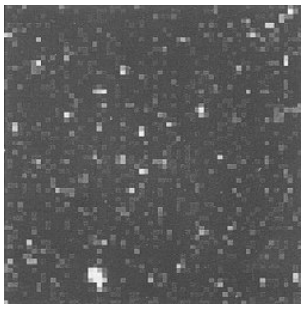
(c) (aii)



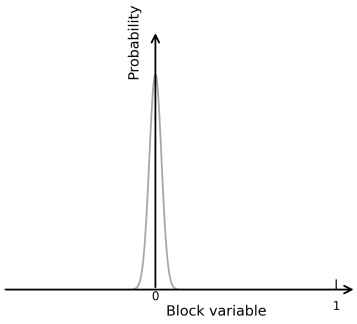
(d) (bii)



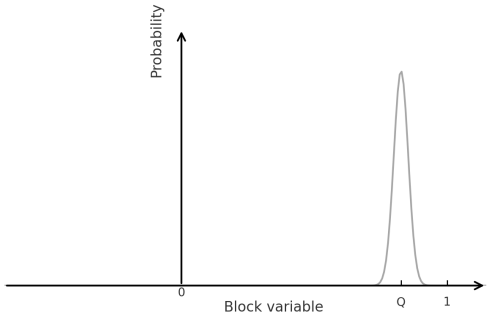
(e) (aiii)



(f) (biii)



(g) (aiv)



(h) (biv)

Figure 7.1: See text for details

variables evolve in time) shows (Figure 7.2(iv)) that it is almost identical to that of the $L = 8$ configurations (given the block variable scaling). The implication of this limiting behaviour is clear: the patterns formed by the ordering variable at criticality look the same (in a statistical sense) when viewed on all sufficiently large length scales.

Let us summarize. Under the coarse-graining operation there is an evolution or *flow* of the system's configuration spectrum. The flow tends to a limit, or fixed point, such that the pattern spectrum does not change under further coarse-graining. These scale-invariant limits have a trivial character for $T > T_c$, (a perfectly disordered arrangement) and $T < T_c$, (a perfectly ordered arrangement). The hallmark of the critical point is the existence of a scale-invariant limit which is neither fully ordered nor fully disordered but which possesses structure on all length scales.

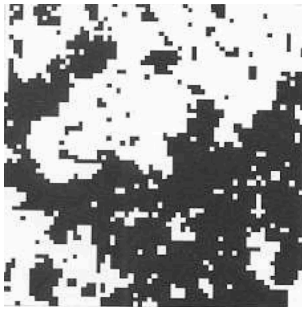
A nice illustration of these points made by my former postdoc Douglas Ashton can be viewed here. (Note this video uses a different coarse-graining scheme called a "majority rule": blocks variables are assigned to be $+1$ or -1 depending on whether spin-up or spin-down is in the majority in the underlying block. Thus in contrast to our scheme, there is no gray scale.)

7.3 Universality and Scaling

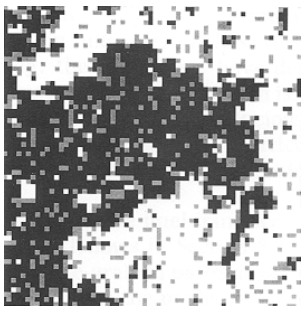
Equipped with the coarse-graining technique, we now address the universality phenomenon. We aim to understand how it is that systems that are different microscopically can nevertheless display critical point behaviour which (in certain respects) is quantitatively identical.

To obtain initial insight we introduce a spin-1 Ising model in which the spins take on three values ($s_i = 1, 0, -1$), in contrast to the two values ($s_i = 1, -1$) of the spin-1/2 Ising model. The two models have properties which are different: for example, T_c for the three-state model is some 30% lower than that of the two-state model (for the same coupling J). However, there is abundant evidence that the two models have the same universal properties.

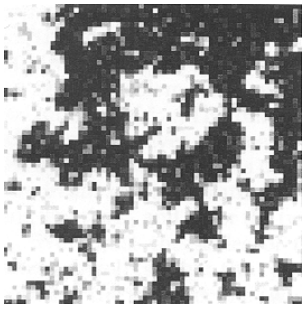
Let us explore what is the same and what is different in the configurations of the two models at criticality. The configurations of the local variables s_i are clearly qualitatively different for the two models. Now consider the coarse-grained configurations (with $L = 4$ and $L = 8$ respectively) for the three-state model at the critical point. We have already seen that the coarse-graining operation bears the configuration spectrum of the critical two-state Ising model to a non-trivial scale-invariant limit. It is scarcely surprising that the same is true for the three-state model. What is remarkable is that the two limits are the same! This is expressed in Figure 7.2(iv), which shows the near coincidence of the distribution of block variables (grey-levels) for the two different coarse-graining lengths. Thus the coarse-graining erases the physical differences apparent in configurations where the local behaviour is resolvable, and exposes a profound configurational similarity.



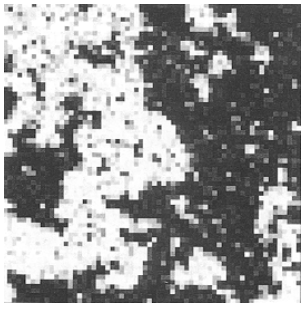
(a) (ai)



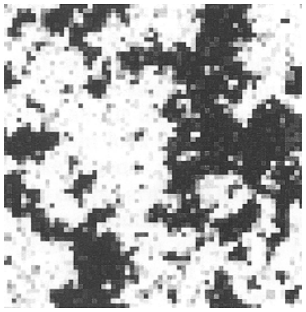
(b) (bi)



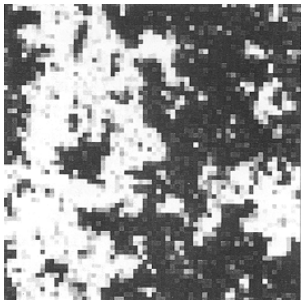
(c) (aii)



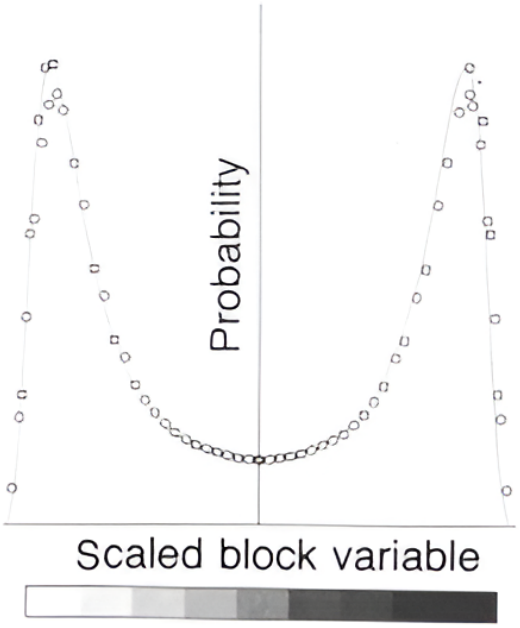
(d) (bii)



(e) (aiii)



(f) (biii)



(g) (iv)

Figure 7.2: See text for details

7.3.1 Fluid-magnet universality

Let us now turn to fluid-magnet universality. In a magnet, the relevant configurations are those formed by the coarse-grained magnetisation (the magnetic moment averaged over a block of side L). In a fluid, the relevant configurations are those of the coarse-grained density (the mass averaged over a block if side L) or more precisely, its fluctuation from its macroscopic average (Figure 7.5). The patterns in the latter (bubbles of liquid or vapour) may be matched to pattern in the former (microdomains of the magnetisation), given appropriate scaling operations to camouflage the differences between the length scales and the differences between the variable scales.

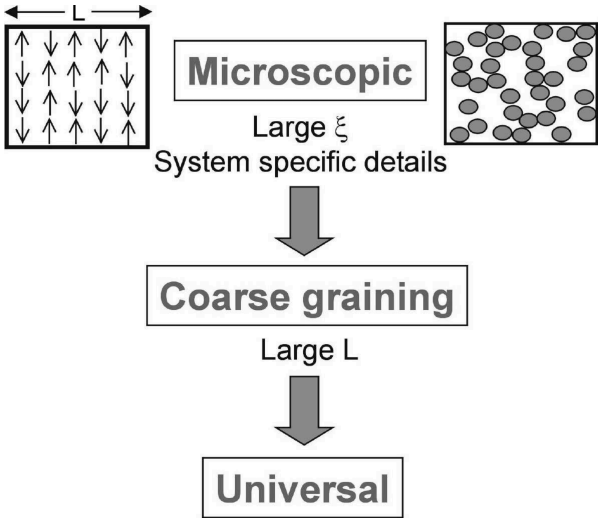


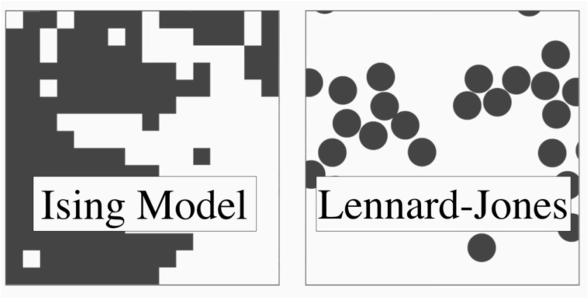
Figure 7.3: Schematic representation of the coarse graining operation via which the universal properties of fluids and magnets may be exposed.

The results is illustrated in Figure 7.4.

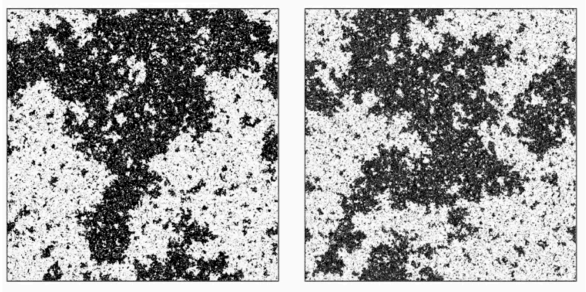
A movie in which we progressively zoom out shows how the loss of microscopic details reveals the large lengthscale universal features. Movies/universality.mov

7.4 Near critical scaling

The similarity of coarse-grained configurations of different systems is not restricted to the critical temperature itself. Suppose we have a two state spin model and a three state spin model each somewhat above their critical points at reduced temperature t. The two systems will have somewhat different correlation lengths, ξ_1 and ξ_2 say. Suppose however, we choose coarse-graining lengths L_1 for L_2 for the two models such that $\xi_1/L_1 = \xi_2/L_2$. We adjust the scales of the block variables (our grey level control) so that the typical variable value is the



(a) 2D critical Ising model and 2d critical Lennard-Jones fluid at small lengthscales



(b) Same models as above, but viewed at large lengthscales

Figure 7.4: Snapshot configurations of the 2D critical Ising model (left) and the 2D critical Lennard-Jones fluid (right). When viewed on sufficiently large length scales the configurational patterns appear universal and self similar.

same for the two systems. We adjust the length scale of the systems (stretch or shrink our snapshots) so that the sizes of the minimum-length-scale structure (set by L_1 and L_2) looks the same for each system. Precisely what they look like depends upon our choice of ξ/L.

7.5 Universality classes

Coarse graining does not erase all differences between the physical properties of critical systems. Differences in the space dimension d of two critical systems will lead to different universal properties such as critical exponents. Thus, for instance, the critical exponents of the 2D magnet, match those of the 2d fluid, but they are different to those of 3d magnets and fluids.

	$d = 2$	$d = 3$
Critical temperature	0.5673	0.75
Order parameter exponent β	$\frac{1}{8}$	0.325 ± 0.001
Susceptibility exponent γ	$\frac{7}{4}$	1.24 ± 0.001
Correlation length exponent ν	1	0.63 ± 0.001

In fact the space dimension is one of a small set of qualitative features of a critical system which are sufficiently deep-seated to survive coarse graining and which together serve to define the system's universal behaviour, or *universality class*. The constituents of this set are not all identifiable *a priori*. They include the number of components n of the order parameter. Up to now, we have only considered order parameters which are scalar (for a fluid the density, for a magnet the magnetisation), for which $n = 1$. In some ferromagnets, the order parameter may have components along two axes, or three axes, implying a vector order parameter, with $n = 2$ (the so called XY model) or $n = 3$ (Heisenberg model), respectively. It is clear that the order-parameter n-value will be reflected in the nature of the coarse-grained configurations, and thus in the universal observables they imply.

A third important feature which can change the universality class of a critical system is the range of the interaction potential between its constituent particles. Clearly for the Ising model, interactions between spins are inherently nearest neighbour in character. Most fluids interact via dispersion forces (such as the Lennard-Jones potential) which is also short ranged owing to the r^{-6} attractive interaction. However some systems have much longer ranged interactions. Notable here are systems of charged particles which interact via a Coulomb potential. The long ranged nature of the Coulomb potential (which decays like r^{-1}) means that charged systems often do not have the same critical exponents as the Ising model and fluid.

7.6 Critical exponents

We have seen that at the critical point the coarse-grained configurations become statistically similar when viewed on sufficiently large length scales. We now relate this scale invariance to the critical exponents.

Recall the bulk critical behaviour, where $t = (T - T_c)/T_c$:

$$\xi \sim |t|^{-\nu}, \qquad Q \sim (-t)^{\beta} \quad (t < 0), \qquad \chi \sim |t|^{-\gamma}.$$

Here Q is the order parameter, and χ is its susceptibility. The exponents describe how these quantities change as the critical point is approached. The essential RG idea is that the same exponents also characterise how the system changes under coarse-graining.

Recall that L denotes the *coarse-graining length*: a block contains L^d microscopic sites. At a temperature close to T_c, the appearance of a coarse-grained configuration depends on the ratio ξ/L. Since $\xi \sim |t|^{-\nu}$, the corresponding dimensionless measure of the distance from criticality is $tL^{1/\nu}$ (apart from a non-universal constant). Thus increasing L at fixed t makes the system appear further from criticality. At $t = 0$, by contrast, there is no finite correlation length to provide such a cutoff.

The typical magnitude of the coarse-grained ordering variable also changes with block size. At criticality it decreases as $L^{-\beta/\nu}$. In the notation used for RG scale factors, these two effects can be summarised as

$$\begin{aligned} a(L) &= a_0 L^{1/\nu}, \\ b(L) &= b_0 L^{\beta/\nu}. \end{aligned} \tag{7.2}$$

The constants a_0 and b_0 depend on microscopic details, whereas the exponents are universal within a universality class. We will not need the full probability distribution of the block variables to use these results.

7.7 Finite-size scaling

An infinite system can have a diverging correlation length and susceptibility at a continuous phase transition. A simulation, however, has a finite linear size, which we denote by $L_{\max}$ to distinguish it from the coarse-graining length L.

As the critical point is approached, ξ grows until it becomes comparable to $L_{\max}$. Beyond this point the finite system cannot reproduce the growth of correlations that would occur in the thermodynamic limit. The critical singularities are therefore rounded. The temperature range over which finite-size effects become important can be estimated from

$$\xi \sim |t|^{-\nu} \sim L_{\max}, \qquad \text{giving} \qquad |t| \sim L_{\max}^{-1/\nu}.$$

This is the basis of *finite-size scaling*. Near the critical point, the dependence of an observable on temperature and system size can be expressed through the combination $tL_{\max}^{1/\nu}$, apart from non-universal scale factors and corrections to scaling.

7.7.1 Finite-size scaling of the susceptibility

In the bulk critical region we have

$$\chi \sim |t|^{-\gamma}, \qquad \xi \sim |t|^{-\nu}.$$

Eliminating $|t|$ gives

$$\chi \sim \xi^{\gamma/\nu}.$$

In a finite system the growth of ξ is cut off when ξ becomes of order $L_{\max}$. The maximum susceptibility therefore scales as

$$\chi_{\max}(L_{\max}) \sim L_{\max}^{\gamma/\nu}. \tag{7.3}$$

This result is especially useful in simulations. By measuring the maximum susceptibility for several system sizes, a log–log plot of $\chi_{\max}$ against $L_{\max}$ has an asymptotic slope γ/ν.

More generally, the susceptibility has the finite-size scaling form

$$\chi(L_{\max}, t) = L_{\max}^{\gamma/\nu} f_\chi(tL_{\max}^{1/\nu}), \tag{7.4}$$

where f_χ is a scaling function. Thus susceptibility curves for different sizes can be compared by plotting $\chi L_{\max}^{-\gamma/\nu}$ against $tL_{\max}^{1/\nu}$. Close to criticality, data for sufficiently large systems should collapse onto a common curve when the correct critical temperature and exponents are used.

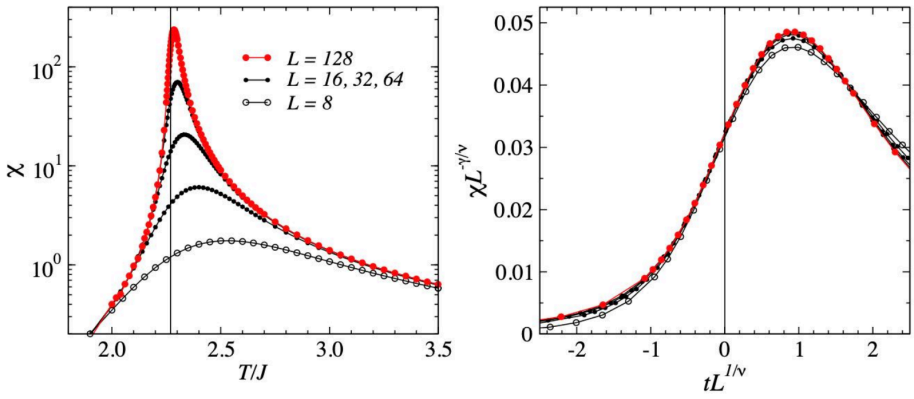


Figure 7.5: Collapse of simulation data for the susceptibility χ on to a master curve under finite-size scaling.

7.7.2 Finite-size scaling of the order parameter

The corresponding scaling form for the magnitude of the order parameter is

$$\langle |m| \rangle = L_{\max}^{-\beta/\nu} f_m(tL_{\max}^{1/\nu}). \tag{7.5}$$

For a finite Ising system in zero applied field, $\langle m \rangle = 0$ by spin-reversal symmetry. This is why we use $\langle |m| \rangle$ (or, equivalently for scaling purposes, $\sqrt{\langle m^2 \rangle}$) rather than $\langle m \rangle$ in this relation. At the critical temperature it follows that

$$\langle |m| \rangle_{T_c} \sim L_{\max}^{-\beta/\nu}.$$

Finite-size scaling therefore provides a practical way to estimate critical exponents from simulations even though no finite system has a true thermodynamic singularity.

7.8 Summary of main points

- Close to criticality, correlations extend over a wide range of length scales. This is why mean-field theory cannot reproduce the full critical behaviour.
- RG progressively coarse-grains the microscopic degrees of freedom. At a critical fixed point, the large-scale statistics are unchanged by further coarse-graining.
- Systems with different microscopic details can belong to the same universality class. Important distinguishing features include the dimensionality, the symmetry of the order parameter and the range of interactions.

- The exponents ν and β describe, respectively, the change in the effective distance from criticality and the scale of the ordering variable under coarse-graining.
- Finite systems cannot support a correlation length much larger than $L_{\max}$. In particular, $\chi_{\max} \sim L_{\max}^{\gamma/\nu}$ and $\langle |m| \rangle_{T_c} \sim L_{\max}^{-\beta/\nu}$. These relations allow critical exponents to be estimated from simulations.

7.9 Addendum: The effective coupling viewpoint of the renormalization group (non examinable)

Notes for those interested in a different perspective on RG theory.

Let us begin by returning to our fundamental Equation 2.1, which we rewrite as

$$p = Z^{-1} e^{-H}$$

where $H \equiv E/k_B T$.
The first step is then to imagine that we generate, by a computer simulation procedure for example, a sequence of configurations with relative probability $\exp(-H)$. We next adopt some coarse-graining procedure which produces from these original configurations a set of coarse-grained configurations. We then ask the question: what is the energy function H' of the coarse-grained variables which would produce these coarse-grained configurations with the correct relative probability $\exp(-H')$? Clearly the form of H' depends on the form of H thus we can write symbolically

$$H' = R(H)$$

The operation R, which defines the coarse-grained configurational energy in terms of the microscopic configurational energy function is known as a renormalisation group transformation (RGT). What it does is to replace a hard problem by a less hard problem. Specifically, suppose that our system is near a critical point and that we wish to calculate its large-distance properties. If we address this task by utilizing the configurational energy and appealing to the basic machinery of statistical mechanics set out in Equation 2.1 and Equation 2.2, the problem is hard. It is hard because the system has fluctuations on all the (many) length scales intermediate between the correlation length ξ and the minimum length scale $L_{\min}$.
However, the task may instead be addressed by tackling the coarse-grained system described by the energy H'. The large-distance properties of this system are the same as the large-distance properties of the physical system, since coarse-graining operation preserves large-scale configurational structure. In this representation the problem is a little easier: while the ξ associated with H' is the same as the ξ associated with H, the minimum length scale of H' is bigger than that of H. Thus the statistical mechanics of

H' poses a not-quite-so-many-length-scale problem, a problem which is effectively a little less critical and is thus a little easier to solve. The benefits accruing from this procedure may be amplified by repeating it. Repeated application of R will eventually result in a coarse- grained energy function describing configurations in which the ξ is no bigger than the minimum length scale. The associated system is far from criticality and its properties may be reliably computed by any of a wide variety of approximation schemes. These properties are the desired large-distance properties of the physical system. As explicit reference to fluctuations of a given scale is eliminated by coarse-graining, their effects are carried forward implicitly in the parameters of the coarse-grained energy.
In order to setup the framework for a simple illustrative example, let is return to the lattice Ising model for which the energy function depended only on the product of nearest neighbour spins. The coefficient of this product in the energy is the exchange coupling, J. In principle, however, other kinds of interactions are also allowed; for example, we may have a product of second neighbour spins with strength J_2 or, perhaps, a product of four spins (at sites forming a square whose side is the lattice spacing), with strength J_3. Such interactions in a real magnet have their origin in the quantum mechanics of the atoms and electrons and clearly depend upon the details of the system. For generality therefore we will allow a family of exchange couplings J_1,J_2,J_3, ..., or $J_a, a = 1, 2, ...$ In reduced units, the equivalent coupling strengths are $K_a = J_a/k_BT$. Their values determine uniquely the energy for any given configuration.

> We note that it is not only useful to allow for arbitrary kinds of interactions: if we wish to repeat the transformation several (indeed many) times, it is also necessary because even if we start with only the nearest neighbour coupling in H the transformation will in general produce others in H'.

Now consider the coarse-graining procedure. Let us suppose that this procedure takes the form of a 'majority rule' operation in which the new spins are assigned values $+1$ or -1 according to the signs of the magnetic moments of the blocks with which they are associated. The new energy function H' will be expressible in terms of some new coupling strengths K' describing the interactions amongst the new spin variables (and thus, in effect, the interactions between blocks of the original spin variables). The RGT simply states that these new couplings depend on the old couplings: K'_1 is some function f_1 of all the original couplings, and generally

$$K'_a = f_a(K_1, K_2, ...) = f_a(\mathbf{K}), \quad a = 1, 2, ... \tag{7.6}$$

where $\mathbf{K}$ is shorthand for the set $K_1, K_2, ...$

7.9.1 A simple example

This example illustrates how one can perform the RG transformation Equation 7.6 directly, without recourse to a 'sequence of typical configurations'. The calculation involves

a very crude approximation which has the advantage that it simplifies the subsequent analysis.

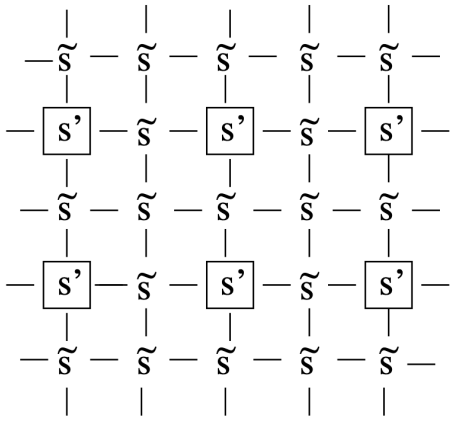


Figure 7.6: Coarse graining by decimation. The spins on the original lattice are divided into two sets $\{s'\}$ and $\{\tilde{s}\}$. The $\{s'\}$ spins occupy a lattice whose spacing is twice that of the original. The effective coupling interaction between the $\{s'\}$ spins is obtained by performing the configurational average over the $\{\tilde{s}\}$

Consider an Ising model in two dimensions, with only nearest neighbour interactions as shown in Figure 7.6. We have divided the spins into two sets, the spins $\{s'\}$ form a square lattice of spacing 2, the others being denoted by $\{\tilde{s}\}$. One then defines an effective energy function H' for the s' spins by performing an average over all the possible arrangements of the $\tilde{s}$ spins

$$\exp(-H') = \sum_{\{\tilde{s}\}} \exp(-H). \tag{7.7}$$

This particular coarse-graining scheme is called 'decimation' because a certain fraction (not necessarily one-tenth!) of spins on the lattice is eliminated. This formulation of a new energy function realizes two basic aims of the RG method: the long-distance physics of the 'original' system, described by H, is contained in that of the 'new' system, described by H' (indeed the partition functions are the same as one can see by summing both sides over s') and the new system is further from critically because the ratio of ξ to lattice spacing ('minimum length scale') has been reduced by a factor of $1/2$ (the ratio of the lattice spacings of the two systems). We must now face the question of how to perform the configuration sum in Equation 7.7. This cannot in general be done exactly, so we must resort to some approximation scheme. The particular approximation which we invoke is the high temperature series expansion. In its simplest mathematical form, since H contains a factor $1/k_BT$, it involves the expansion of $\exp(-H)$ as a power series:

$$\exp(-H/k_BT) = 1 - H/k_BT + \frac{1}{2!}(H/k_BT)^2 + ...$$

We substitute this expansion into the right hand side of Equation 7.7 and proceed to look for terms which depend on the s' spins after the sum over the possible arrangements of the $\tilde{s}$ spins is performed. This sum extends over all the possible (± 1) values of all the $\tilde{s}$ spins. The first term (the 1) in the expansion of the exponential is clearly independent of the values of the s' spins. The second term (H) is a function of the s' spins, but gives zero when the sum over the s' spins is performed because only a single factor of any s' ever appears, and $+1-1=0$. The third term ($H^2/2$) does contribute. If one writes out explicitly the form of $H^2/2$ one finds terms of the form $K^2 s'_1 \tilde{s}\tilde{s} s'_2 = K^2 s'_1 s'_2$, where s'_1 and s'_2 denote two spins at nearest neighbour sites on the lattice of s' spins and $\tilde{s}$ is the spin (in the other set) which lies between them. Now, in the corresponding expansion of the left hand side of Equation 7.7, we find terms of the form $K' s'_1 s'_2$, where K' is the nearest neighbour coupling for the s' spins. We conclude (with a little more thought than we detail here) that

$$K' = K^2 \tag{7.8}$$

Of course many other terms and couplings are generated by the higher orders of the high temperature expansion and it is necssary to include these if one wishes reliable values for the critical temperature and exponents, However, our aim here is to use this simple calculation to illustrate the RG method. Let us therefore close our eyes, forget about the higher order terms and show how the RGT Equation 7.8 can be used to obtain information on the phase transition.

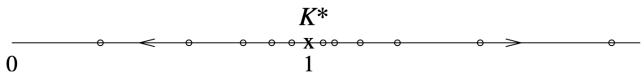


Figure 7.7: Coupling flow under the decimation transformation described in the text.

The first point to note is that that mathematically Equation 7.8 has the fixed point $K^* = 1$; if $K = 1$ then the new effective coupling K' has the same value 1. Further, if K is just larger than 1, then K' is larger than K, i.e. further away from 1. Similarly, if K is less than 1, K' is less than K. We say that the fixed point is unstable: the flow of couplings under repeated iteration of Equation 7.8 is away from the fixed point, as illustrated in Figure 7.7. The physical significance of this is as follows: suppose that the original system is at its critical point so that the ratio of ξ to lattice spacing is infinite. After one application of the decimation transformation, the effective lattice spacing has increased by a factor of two, but this ratio remains infinite; the new system is therefore

also at its critical point. Within the approximations inherent in Equation 7.8, the original system is an Ising model with nearest neighbour coupling K and the new system is an Ising model with nearest neighbour coupling K'. If these two systems are going to be at a common criticality, we must identify $K' = K$. The fixed point $K^* = 1$ is therefore a candidate for the critical point K_c, where the phase transition occurs. This interpretation is reinforced by considering the case where the original system is close to, but not at, criticality. Then ξ is finite and the new system is further from critically because the ratio of ξ to lattice spacing is reduced by a factor of two. This instability of a fixed point to deviations of K from K^* is a further necessary condition for its interpretation as a critical point of the system. In summary then we make the prediction

$$K_c = J/k_B T_c = 1 \tag{7.9}$$

We can obtain further information about the behaviour of the system close to its critical point. In order to do so, we rewrite the transformation (Equation 7.8) in terms of the deviation of the coupling from its fixed point value. A Taylor expansion of the function $K' = K^2$ yields

$$\begin{aligned} K' =& (K^*)^2 + (K - K^*) \left.\frac{\partial K'}{\partial K}\right|_{K=K^*} + \frac{1}{2}(K - K^*)^2 \left.\frac{\partial^2 K'}{\partial K^2}\right|_{K=K^*} + \ldots \\ K' - K^* =& 2(K - K^*) + (K - K^*)^2 \end{aligned}$$

where in the second line we have used the fact that the first derivative evaluates to $2K^* = 2$ and $(K^*)^2 = K^*$.
For a system sufficiently close to its critical temperature the final term can be neglected. The deviation of the coupling from its fixed point (critical) value is thus bigger for the new system than it is for the old by a factor of two. This means that the reduced temperature is also bigger by a factor of two:

$$t' = 2t$$

But ξ (in units of the appropriate lattice spacing) is smaller by a factor of 1/2:

$$\xi' = \xi/2$$

Thus, when we double t, we halve ξ, implying that

$$\xi \propto t^{-1}$$

for T close to T_c. Thus we see that the RGT predicts scaling behaviour with calculable critical exponents. In this simple calculation we estimate the critical exponent $\nu = 1$ for the square lattice Ising model. This prediction is actually in agreement with the exactly established value. The agreement is fortuitous- the prediction in Eq. refeq:Kc for K_c, is

larger than the exactly established value by a factor of more than two. In order to obtain reliable estimates more sophisticated and systematic methods must be used.
The crude approximation in the calculation above produced a transformation, Equation 7.8, involving only the nearest neighbour coupling, with the subsequent advantages of simple algebra. We pay a penalty for this simplicity in two ways: the results obtained for critical properties are in rather poor agreement with accepted values, and we gain no insight into the origin of universality.

7.9.2 Universality and scaling

In order to expose how universality can arise, we should from the start allow for several different kinds of coupling J_a, and show how the systems with *different* J_a can have the *same* critical behaviour.

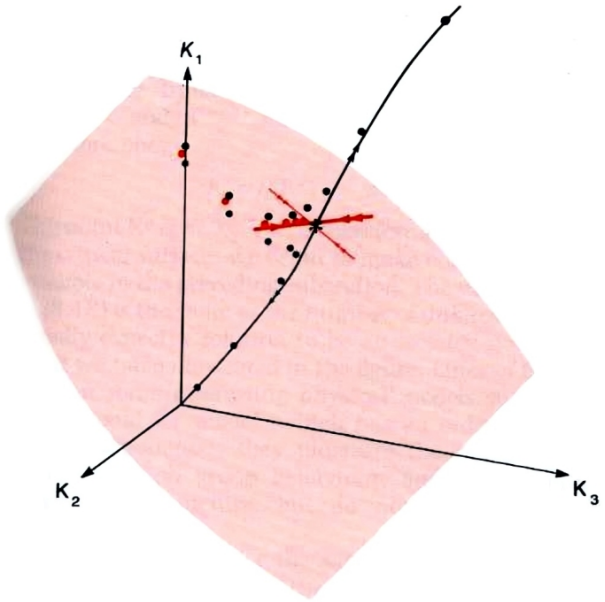


Figure 7.8: General flow in coupling space

Figure 7.8 is a representation of the space of all coupling strengths K_a in the energy function H/k_BT. This is of course actually a space of infinite dimension, but representing three of these, as we have done, enables us to illustrate all the important aspects. First let us be clear what the points in this space represent. Suppose we have some magnetic material which is described by a given set of exchange constants J_1, J_2, J_3..... As the temperature T varies, the coupling strengths $K_a = J_a/k_BT$ trace out a straight line, or ray, from the origin of the space in the direction $(J_1, J_2, J_3....)$. Points on this ray

close to the origin represent this magnet at high temperatures, and conversely points far from the origin represent the magnet at low temperatures. The critical point of the magnet is represented by a specific point on this ray, $K_a = J_a/k_BT, a = 1, 2, ...$ The set of critical points on all of the possible rays forms a *surface*, the critical surface. Formally, it is defined by the set of all possible models (of the Ising type) which have infinite ξ. It is shown schematically as the shaded surface in Figure 7.8. (In the figure it is a two-dimensional surface; more generally it has one dimension less than the full coupling constant space, dividing all models into high and low temperature phases.)

Our immediate goal then is to understand how the RGT can explain why different physical systems near this critical surface have the same behaviour. Let us turn now to the schematic representation of the RG flow in Figure 7.8. Suppose we start with a physical system, with coupling strengths $K_a, a = 1, 2, ...$ What the RGT does is generate a new point in the figure, at the coupling strengths $K_a^{(1)} = f_a(\mathbf{K})$; these are the couplings appearing in the effective energy function describing the coarse-grained system. If we repeat the transformation, the new energy function has coupling strengths $K_a^{(2)} = f_a(\mathbf{K})$. Thus repeated application of the transformation generates a flow of points in the figure: $\mathbf{K} \to K^{(1)} \to ... \to K^{(n)}$ where the superscript (n) labels the effective couplings after n coarse-graining steps. if the change in coarse-graining scale is b (> 1) at each step, the total change in coarse-graining scale is b^n after n steps. In the process, therefore, the ratio of ξ to coarse-graining scale is reduced by a factor of b^{-n}. The dots in Figure 7.8 identify three lines of RG flow starting from three systems differing only in their temperature. (The flow lines are schematic but display the essential features revealed in detailed calculations.)

Consider first the red dots which start from the nearest neighbour Ising model at its critical point. The ratio of ξ to coarse-graining scale is reduced by a factor b at each step, but, since it starts infinite, it remains infinite after any finite number of steps. In this case we can in principle generate an unbounded number of dots, $\mathbf{K^{(1)}}, \mathbf{K^{(2)}}, ..., \mathbf{K^{(n)}}$, all of which lie in the critical surface. The simplest behaviour of such a sequence as n increases is to tend to a limit, K^*, say. In such a case

$$K_a^* = f_a(K^*) \qquad a = 1, 2.....$$

This point $\mathbf{K}^* \equiv K_1^*, K_2^*, ...$ is therefore a *fixed point* which lies in the critical surface.

By contrast, consider the same magnet as before, now at temperature T just greater than T_c, its couplings K_a, will be close to the first red dot (in fact they will be slightly smaller) and so will the effective couplings $K_a^{(1)}, K_2^{(2)}, ...$ of the corresponding coarse-grained systems. The new flow will therefore appear initially to follow the red dots towards the same fixed point. However, the flow must eventually move away from the fixed point because each coarse-graining now produces a model further from criticality. The resulting flow is represented schematically by one set of black dots. The other set of black dots shows the expected flow starting from the same magnet slightly below its critical temperature.

We are now in a position to understand both universality and scaling within this framework. We will suppose that there exists a single fixed point in the critical surface which sucks in all flows starting from a point in that surface. Then any system at its critical point will exhibit large-length scale physics (large-block spin behaviour) described by the single set of fixed point coupling constants. The uniqueness of this limiting set of coupling constants is the essence of critical point universality. It is, of course, the algebraic counterpart of the unique limiting spectrum of coarse-grained configurations, discussed in Section 7.5. Similarly the scale-invariance of the critical point configuration spectrum (viewed on large enough length scales) is expressed in the invariance of the couplings under iteration of the transformation (after a number of iterations large enough to secure convergence to the fixed point).

To understand the behaviour of systems near but not precisely at critically we must make a further assumption (again widely justified by explicit studies). The flow line stemming from any such system will, we have argued, be borne towards the fixed point before ultimately deviating from it after a number of iterations large enough to expose the system's noncritical character. We assume that (as indicated schematically in the streams of red and blue lines in Figure 7.8 the deviations lie along a single line through the fixed point, the direction followed along this line differing according to the sign of the temperature deviation $T - T_c$. Since any two sets of coupling constants on the line (on the same side of the fixed point) are related by a suitable coarse-graining operation, this picture implies that the large-length-scale physics of all near- critical systems differs only in the matter of a length scale. This is the essence of near-critical point universality.

8 Introduction to stochastic processes

Many natural phenomena are stochastic — they involve randomness in their evolution over time.

In classical physics, this randomness may arise from our lack of knowledge about microscopic details. For example, in a gas, we do not know the precise positions and velocities of each particle, so their collisions with the container walls appear random.

In quantum mechanics, stochasticity is even more intrinsic. The fundamental objects are probability amplitudes, and outcomes are inherently probabilistic.

To describe these systems effectively, we use a coarse-grained probabilistic description, which tracks the likelihood of different outcomes rather than precise trajectories. One of the key tools in this approach is the master equation.

8.1 The Master Equation

Consider a system in microstate i with energy E_i. It can transition to neighboring microstates j, where the energy difference $|E_j - E_i|$ is small (within δE).

Let ν_{ij} be the **rate** at which the system jumps from state i to state j. Over an infinitesimal time interval dt, the probability p_i changes as:

$$dp_i = \left[-p_i \sum_j \nu_{ij} + \sum_j \nu_{ji} p_j \right] dt$$

This expression contains two terms:

- A *loss term*: the system leaves state i at rate ν_{ij},
- A *gain term*: the system arrives in state i from other states j at rate ν_{ji}.

The master equation becomes:

$$\frac{dp_i}{dt} = -\sum_j \nu_{ij} p_i + \sum_j \nu_{ji} p_j$$

This is a linear first-order differential equation for the vector of probabilities $\{p_i\}$.

Alternatively, in matrix form:

$$\frac{d\mathbf{p}}{dt} = W\mathbf{p}$$

where W is the **rate matrix** with entries:

- $W_{ij} = \nu_{ji}$ for $i \neq j$,
- $W_{ii} = -\sum_{j \neq i} \nu_{ij}$.

This structure ensures probability conservation: the total probability $\sum_i p_i = 1$ remains constant in time.

> An aside on entropy production
>
> The master equation is first order in time and does not have time reversal symmetry so describes an irreversible process. This irreversibility arises from the coarse-graining process that throws away information about underlying microphysics which is described by Newton's equations and which *are* time reversible. Only by doing so is the entropy allowed to increase which is required by the second law of thermodynamics for an irreversible process. Consequently the increase of entropy is linked to our knowledge about the system rather than anything it is doing internally in a manner that may appear dubious. Can it be possible that macroscopic and reproducible phenomena such as heat flow depend on how we handle information? Perhaps yes since the division between work and heat is somewhat arbitrary. Were we able to track all the particle positions there would be no need to talk about heat energy or heat flow.

8.2 From the Master Equation to the Diffusion Equation

Now consider the situation where the state index i corresponds to a position in space, $x_i = ia$, ie a one-dimensional lattice with lattice spacing a, and transitions only occur between neighboring lattice sites. The situation is illustrated schematically in Figure 8.1.

We assume:

- Transition rates are symmetric: $\nu_{i,i+1} = \nu_{i,i-1} = \nu$,
- The spacing $a \to 0$ in the continuum limit.

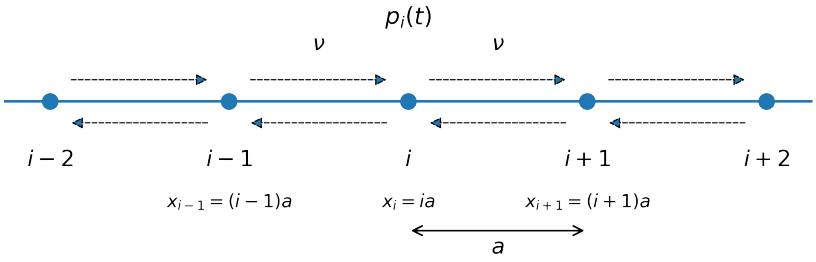


Figure 8.1: Schematic of the one-dimensional lattice random walk with nearest-neighbour transitions at rate ν.

The master equation becomes a finite-difference equation:

$$\begin{aligned}\frac{dp_i}{dt} &= \sum_j \nu_{ij}(p_j - p_i) \\ \frac{dp_i}{dt} &= \nu(p_{i-1} - p_i) + \nu(p_{i+1} - p_i) \\ \frac{dp_i}{dt} &= \nu(p_{i+1} + p_{i-1} - 2p_i)\end{aligned}$$

We now define a continuous variable $x = ia$, and a probability density $p(x,t)$ such that $p_i(t) \approx p(x,t)$.

Using Taylor expansions:

$$p(x \pm a, t) = p(x,t) \pm a\frac{\partial p}{\partial x} + \frac{a^2}{2}\frac{\partial^2 p}{\partial x^2} + \cdots$$

Substituting into the master equation gives:

$$\frac{\partial p}{\partial t} = \nu a^2 \frac{\partial^2 p}{\partial x^2}$$

Defining the diffusion constant $D = \nu a^2$, we obtain the **diffusion equation**:

$$\frac{\partial p}{\partial t} = D\frac{\partial^2 p}{\partial x^2}$$

The diffusion equation describes the evolution of the probability density of a particle with diffusion constant (sometimes called diffusivity) given by $D = \nu a^2$. The dimensions of D are [length]^2/[time]. Typically, after expansion, we set the lattice spacing a to 1. Additionally, the

diffusion equation can describe many non-interacting diffusing particles. In this case, we replace p with ρ, representing the density or concentration of particles, and use the normalization $\int dx\, \rho = M$, where M is the number of particles.

The diffusion equation, much like the master equation from which it originates, explicitly violates time-reversal symmetry, thus permitting entropy to increase.

The solution of the diffusion equation for an initial condition where the particle is initially localized at the origin (formally, $p(x,0) = \delta(x)$) is a Gaussian:

$$p(x,t) = (4\pi D t)^{-1/2} \exp\left[-\frac{x^2}{4Dt}\right]$$

We explicitly see the arrow of time by examining this Gaussian solution at various times t. As t increases, the Gaussian "bell-shaped" curve spreads out. Its width grows according to $\langle x^2 \rangle^{1/2} \sim t^{1/2}$. This is known as "diffusive scaling," and it implies that, after time t, a particle will typically be found at a distance roughly proportional to $t^{1/2}$ from its starting point. Conversely, exploring a region of size L typically requires a time of order $O(L^2)$.

The evolution of the solution to the 1d diffusion equation in a spatial region $x = [0, 1]$ as a function of times are shown in the movie below. The diffusion constant is $D = 0.01$. The movie corresponds to a particle initialised at $x = 0.5$. One sees how the probability density spreads out over the range as time increases. This can be used to model the diffusion of particles down a concentration gradient as you will see in the next part of the course.

Movies/diffusion_evolution.mp4

```
import numpy as np
import matplotlib.pyplot as plt
import matplotlib.animation as animation
import os

# Parameters
L = 1.0        # Length of the domain
T = 1.0        # Total time
nx = 400       # Number of spatial points
nt = 2000      # Number of time steps
D = 0.1        # Diffusion coefficient

# Discretization
dx = L / (nx - 1)
dt = T / nt

# Stability condition auto-adjust
```

```
if D * dt / dx**2 > 0.5:
    print("Adjusting dt and nt to satisfy stability condition...")
    dt = 0.4 * dx**2 / D
    nt = int(T / dt)
    dt = T / nt  # Recalculate dt exactly

nt = int(nt / 50)  # Artificial slowdown for animation

print(f"Using dt = {dt:.4e}, nt = {nt}")

# Initialize x and u
x = np.linspace(0, L, nx)

# Initial condition: smooth narrow Gaussian
sigma = 0.01
u = np.exp(-(x - L/2)**2 / (2 * sigma**2))

# Normalize initial condition
u /= np.sum(u) * dx

# Setup figure
plt.rcParams.update({
    "text.usetex": True,
    "font.family": "serif"
})

fig, ax = plt.subplots()
line, = ax.plot(x, u)

# Compute peak height for setting y-axis
peak_height = 1 / (np.sqrt(2 * np.pi) * sigma)
ax.set_ylim(0, peak_height * 1.05)

ax.set_xlabel(r'$x$', fontsize=20)
ax.set_ylabel(r'$p(x,t)$', fontsize=20)

ax.tick_params(axis='both', which='major', labelsize=14)

# Tiny time counter text
time_text = ax.text(0.85, 0.05, '', transform=ax.transAxes, fontsize=10, verticalalignment='
```

```
# Function to update the plot
def update(frame):
    global u
    unew = np.copy(u)
    unew[1:-1] = u[1:-1] + D * dt / dx**2 * (u[2:] - 2*u[1:-1] + u[:-2])
    u = unew

    # Normalize at every step
    u /= np.sum(u) * dx

    line.set_ydata(u)
    current_time = frame * dt
    time_text.set_text(r'$t=%.4f$' % current_time)
    return line, time_text

ani = animation.FuncAnimation(fig, update, frames=nt, interval=100, blit=True)


# Save the animation as a movie
Writer = animation.writers['ffmpeg']
writer = Writer(fps=15, metadata=dict(artist='Me'), bitrate=1800)
ani.save("../Movies/diffusion_evolution.mp4", writer=writer)


plt.show()
```

8.3 Consequences of time reversal symmetry

As we have seen by introducing a type of coarse graining, the master equation violates time reversal symmetry of the underlying Newtonian dynamics. Remarkably however, the fact that the underlying microphysics is actually time reversal symmetric has several deep consequences which survive the coarse graining procedure These results are some of the cornerstones of nonequilibrium thermodynamics

8.3.1 Detailed balance

Recall from year 2 Statistical Mechanics that for a system in equilibrium, the principle of equal a-priori probabilities of microstates holds. Therefore

$$\nu_{ij} p_i^{eq} = \nu_{ji} p_j^{eq}$$

Hence, on average, the actual rate of quantum jumps from i to j (the left-hand side) is the same as from j to i. This is a stronger statement than the master equation, which asserts only that there is overall balance between the rate of jumping into and out of state i in equilibrium. The result above is known as the *principle of detailed balance*.

This principle is powerful because it applies not only to individual states but also to any grouping of states.

Exercise: Show that for two groups of states, A and B, the overall rate of transitions from group A to group B is balanced, in equilibrium, by those from B to A:

$$\nu_{AB} p_A^{eq} = \nu_{BA} p_B^{eq}$$

Hence, detailed balance arguments can be extended to subsystems within a large isolated system, and even to systems that are not isolated. However, in such cases, the principle is far from obvious, because once states are grouped together:

$$\nu_{AB} \neq \nu_{BA}, \quad p_A \neq p_B$$

(This can be easily demonstrated, for example, by considering two groups that contain different numbers of states with similar energies.) Nonetheless, the detailed balance relation holds, in equilibrium, in the general form above.

8.3.2 Computer simulation

In computer simulation, good results will be obtained if one accurately follows the microscopic equations of motion. This is the *molecular dynamics (MD)* method which we now outline.

Molecular dynamics

Molecular Dynamics (MD) involves a system of classical particles interacting through specified interparticle forces. The motion of these particles is determined by numerically integrating Newton's equations of motion. In MD simulations, averages of state variables are obtained as time averages over trajectories in phase space. Typically, the forces acting between particles are conservative, ensuring that the total energy E remains constant. This conservation implies that the motion is restricted to a $(2dN-1)$-dimensional surface in phase space, denoted by $\Gamma(E)$.

A central aspect of MD is the averaging of observables. For a given observable A, its average is computed as the time average along the trajectory. Mathematically, this is expressed as:

$$\langle A(\{\mathbf{p}_i\},\{\mathbf{r}_i\})\rangle = \frac{1}{\tau}\int_{t_0}^{t_0+\tau} dt\, A(\{\mathbf{p}_i(t)\},\{\mathbf{r}_i(t)\})$$

This formula represents the integral of the observable over a time interval τ, normalized by the length of that interval.

The practical steps of an MD simulation start with generating an initial random configuration of particle positions $\{\mathbf{r}_i\}$ and momenta $\{\mathbf{p}_i\}$. The system's equations of motion are then iteratively solved using a suitable algorithm to allow it to reach equilibrium. After equilibration, a production run is performed over many time steps to collect meaningful data. Finally, relevant averages, such as pressure or kinetic energy, are calculated from the collected data.

Monte Carlo

However, to obtain the equilibrium properties of the system, it may be much faster to use a dynamics which is nothing like the actual equations of motion.

At first sight, this looks very dangerous; however, if one can prove that in the required equilibrium distribution, the artificial dynamics obey the principle of detailed balance, then it is (almost) guaranteed that the steady state found by simulation is the true equilibrium state.

The best known example is the *Monte Carlo method*, in which the dynamical algorithm consists of random jumps. The jump rates ν_{AB} for all pairs of states (A, B) take the form:

$$\nu_{AB} = \nu_0 \quad \text{if } E_B \leq E_A$$

$$\nu_{AB} = \nu_0 e^{-\beta(E_B - E_A)} \quad \text{if } E_B \geq E_A$$

where ν_0 is a constant.

Exercise: Show that this gives the canonical distribution in steady state.

Solution

To show that this jump rate rule gives the canonical distribution in steady state, we assume the system reaches a steady-state probability distribution P_A for state A and apply the condition of detailed balance.
Detailed balance requires:

$$P_A \nu_{AB} = P_B \nu_{BA}$$

Assume the canonical distribution:

$$P_A = \frac{1}{Z} e^{-\beta E_A}, \quad P_B = \frac{1}{Z} e^{-\beta E_B}$$

Now consider two cases for ν_{AB} and ν_{BA}:

Case 1: $E_B \leq E_A$
Then:

$$\nu_{AB} = \nu_0, \quad \nu_{BA} = \nu_0 e^{-\beta(E_A - E_B)}$$

Substitute into the detailed balance condition:

$$P_A \nu_0 = P_B \nu_0 e^{-\beta(E_A - E_B)}$$

Cancel ν_0:

$$P_A = P_B e^{-\beta(E_A - E_B)}$$

Use canonical form:

$$\frac{1}{Z} e^{-\beta E_A} = \frac{1}{Z} e^{-\beta E_B} e^{-\beta(E_A - E_B)} = \frac{1}{Z} e^{-\beta E_A}$$

Verified.
Case 2: $E_B > E_A$
Then:

$$\nu_{AB} = \nu_0 e^{-\beta(E_B - E_A)}, \quad \nu_{BA} = \nu_0$$

Substitute:

$$P_A \nu_0 e^{-\beta(E_B - E_A)} = P_B \nu_0$$

Cancel ν_0:

$$P_A e^{-\beta(E_B - E_A)} = P_B$$

Again using canonical form:

$$\frac{1}{Z} e^{-\beta E_A} e^{-\beta(E_B - E_A)} = \frac{1}{Z} e^{-\beta E_B} = P_B$$

Verified.
Hence, in both cases the detailed balance condition is satisfied with the canonical distribution, and the steady state is indeed the canonical distribution.

9 The Langevin Approach

9.1 The Random Walk and the Langevin equation

The concept of a random walk and its continuum limit – diffusion – introduced in the previous chapter, expresses the time evolution of the probability distribution $p(x,t)$ for a particle's position x by the diffusion equation:

$$\frac{\partial p}{\partial t} = D\frac{\partial^2 p}{\partial x^2},$$

which is a standard example of a so called *Fokker-Planck* equation, which is second-order in space and first-order in time.

In contrast, the *Langevin equation* provides a stochastic differential equation for the particle's trajectory $x(t)$. To understand it, consider the random hopping motion of a particle on a 1d lattice over a small time increment Δt:

$$x(t+\Delta t) = x(t) + \Delta x(t)$$

Here, $\Delta x(t)$ is a random displacement. If the lattice spacing is a, we define the step statistics as:

$$\Delta x(t) = \begin{cases} +a & \text{with probability } \nu\Delta t \\ -a & \text{with probability } \nu\Delta t \\ 0 & \text{with probability } 1-2\nu\Delta t \end{cases}$$

This defines a discrete-time, discrete-space random walk. The average and variance of the step are easily derived (try as an exercise):

- Mean: $\langle \Delta x \rangle = 0$
- Variance: $\langle (\Delta x)^2 \rangle = 2a^2\nu\Delta t = 2D\Delta t$

Solution

The mean displacement is

$$\langle \Delta x \rangle = (+a)(\nu \Delta t) + (-a)(\nu \Delta t) + 0(1 - 2\nu \Delta t) = 0.$$

The mean square displacement is

$$\langle (\Delta x)^2 \rangle = (+a)^2(\nu \Delta t) + (-a)^2(\nu \Delta t) + 0^2(1 - 2\nu \Delta t) = 2a^2 \nu \Delta t.$$

Hence the variance is

$$\mathrm{Var}(\Delta x) = \langle (\Delta x)^2 \rangle - \langle \Delta x \rangle^2 = 2a^2 \nu \Delta t.$$

Identifying $D = a^2 \nu$, we obtain

$$\langle (\Delta x)^2 \rangle = 2D \Delta t.$$

The steps $\Delta x(t)$ are independent over different time intervals. In the continuum limit we represent these random increments by a noise $\eta(t)$:

$$\dot{x}(t) = \eta(t).$$

Since the increments are independent, the noise is uncorrelated at different times:

$$\langle \eta(t) \rangle = 0,$$

$$\langle \eta(t) \eta(t') \rangle = \Gamma \, \delta(t - t').$$

This is called *white noise*. The amplitude Γ will be related below to the diffusion constant D.

The Langevin equation tells us that the velocity $\dot{x}(t)$ is purely driven by noise. We can formally integrate it:

$$x(t) - x_0 = \int_0^t \eta(t') \, dt'$$

Taking ensemble averages, i.e. averaging over all possible realisations of the noise:

- Mean displacement:
$$\langle x(t) - x_0 \rangle = 0$$

- Mean square displacement:

$$\langle [x(t) - x_0]^2 \rangle = \int_0^t \int_0^t \langle \eta(t')\eta(t'') \rangle \, dt' \, dt'' = \Gamma \int_0^t dt' = \Gamma t$$

Comparing this with the diffusion equation result, we identify:

$$\Gamma = 2D$$

Hence, the Langevin description yields the same physical behavior — not just the mean-square displacement but also the full probability distribution $p(x, t)$ — as the diffusion (Fokker-Planck) equation. This equivalence arises from the fact that the integral of many small, independent random steps leads to a Gaussian distribution, in agreement with the solution of the diffusion equation.

For more details, see: *Stochastic Processes in Physics and Chemistry* by N.G. van Kampen (North Holland, 1981).

9.2 Brownian Motion

Let us now examine Brownian motion, originally observed as the erratic motion of colloidal particles suspended in a fluid. The particles undergo continual collisions with the surrounding, much smaller, fluid molecules, producing apparently random motion.

From a coarse-grained perspective, where we do not track each individual molecular collision, these microscopic interactions can be represented by a fluctuating random force. This statistical description introduces an effectively irreversible dynamics at the macroscopic level, even though the underlying molecular dynamics are reversible.

For a Brownian particle of mass m moving in one dimension, Langevin proposed

$$m\ddot{x} = -\gamma\dot{x} + f(t).$$

Here:

- $-\gamma\dot{x}$ is a frictional damping force, with damping coefficient γ.
- $f(t)$ is the fluctuating force arising from molecular collisions.

The term $m\ddot{x}$ represents the particle's inertia: because the particle has a finite mass, its velocity cannot change instantaneously in response to the random force.

Relation to the previous Langevin equation

Earlier, starting from a random walk, we obtained the simpler Langevin equation

$$\dot{x} = \eta(t).$$

This describes the motion on timescales for which the particle's velocity has already relaxed and its inertia can be neglected.
From the full Langevin equation, the characteristic timescale for the velocity to relax is

$$\tau = \frac{m}{\gamma}.$$

For times $t \gg \tau$, the inertial term $m\ddot{x}$ can be neglected, giving

$$\gamma\dot{x} = f(t),$$

or

$$\dot{x} = \frac{f(t)}{\gamma}.$$

Identifying

$$\eta(t) = \frac{f(t)}{\gamma},$$

we recover the Langevin equation obtained from the random-walk description. Thus $\dot{x} = \eta(t)$ is the **overdamped**, or long-time, limit of the more complete Langevin equation.

Often, the mobility is defined as $\mu = 1/\gamma$ — note that this is unrelated to chemical potential.

9.2.1 Noise Properties

In principle the random forces are correlated in time since the molecular collisions which cause them are correlated and have some definite duration.

Let us assume that there is some correlation time t_c over which $\langle f(t_1)f(t_2)\rangle = g(t_1 - t_2)$ decays rapidly as shown in the sketch below:

Then as long as we consider timescales $\gg t_c$ we can safely replace $g(t_1 - t_2)$ by a delta function. Thus we can make the approximation of white noise

$$\langle f(t)\rangle = 0$$

$$\langle f(t_1)f(t_2)\rangle = \Gamma\delta(t_1 - t_2)$$

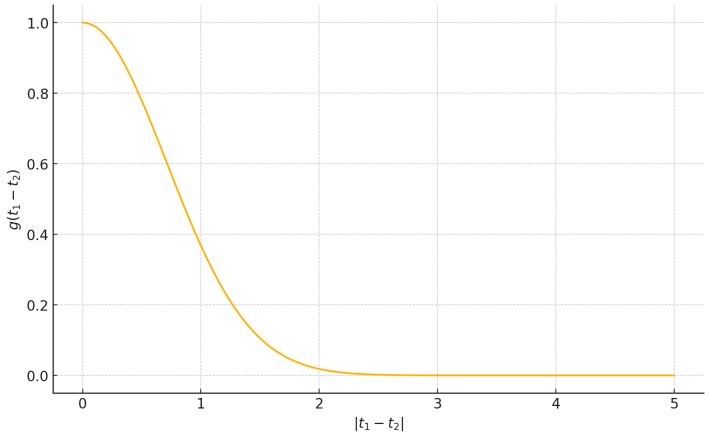


Figure 9.1: Sketch of $g(t_1 - t_2)$ against $|t_1 - t_2|$

9.2.2 Solving the Langevin Equation (velocity)

Let's set $m = 1$ for simplicity and solve the equation:

$$\dot{v} + \gamma v = f(t)$$

We apply an integrating factor to get an exact differential on the LHS:

$$\frac{d}{dt}\left[ve^{\gamma t}\right] = e^{\gamma t} f(t)$$

Integrating both sides:

$$\int_0^t \frac{d}{dt'}\left(ve^{\gamma t'}\right) dt' = \int_0^t e^{\gamma t'} f(t')\, dt'$$

$$v(t)e^{\gamma t} - v_0 = \int_0^t e^{\gamma t'} f(t')\, dt'$$

$$v(t) = v_0 e^{-\gamma t} + \int_0^t e^{-\gamma(t-t')} f(t')\, dt'$$

We now averaging over all possible realisations of the random force, i.e we imagine repeating the Brownian motion experiment infinitely many times, each with a different random sequence of microscopic kicks $f(t)$. Then

$$\langle v(t)\rangle = v_0 e^{-\gamma t}$$

where we have used the fact that $f(t)$ is random with $\langle f(t)\rangle = 0$. Thus:

- At short times: ($\gamma t \ll 1$): $\langle v\rangle \approx v_0$ ie. friction is negligible.
- At long times: ($\gamma t \gg 1$): $\langle v\rangle \to 0$ ie. the system loses memory of the initial velocity.

9.2.3 Mean-square velocity

We now compute (try it as an exercise):

$$\langle v(t)^2\rangle = v_0^2 e^{-2\gamma t} + \Gamma \int_0^t e^{-2\gamma(t-t')} dt' = v_0^2 e^{-2\gamma t} + \frac{\Gamma}{2\gamma}\left(1 - e^{-2\gamma t}\right)$$

Solution

From the solution for $v(t)$ with $m = 1$:

$$v(t) = v_0 e^{-\gamma t} + \int_0^t e^{-\gamma(t-t')} f(t')\, dt'.$$

$$\Rightarrow\ v(t)^2 = v_0^2 e^{-2\gamma t} + 2v_0 e^{-\gamma t} \int_0^t e^{-\gamma(t-t')} f(t')\, dt' + \int_0^t \int_0^t e^{-\gamma(2t-t'-t'')} f(t') f(t'$$

$$\Rightarrow\ \langle v(t)^2\rangle = v_0^2 e^{-2\gamma t} + 2v_0 e^{-\gamma t} \int_0^t e^{-\gamma(t-t')} \underbrace{\langle f(t')\rangle}_{=0}\, dt' + \int_0^t \int_0^t e^{-\gamma(2t-t'-t'')} \underbrace{\langle f(t') f(t'')\rangle}_{=\Gamma\,\delta(t'-t'')}\, dt'\, dt''$$

$$= v_0^2 e^{-2\gamma t} + \Gamma \int_0^t e^{-2\gamma(t-t')}\, dt'$$

$$= v_0^2 e^{-2\gamma t} + \Gamma \left[\frac{1}{2\gamma} e^{-2\gamma(t-t')}\right]_{t'=0}^{t'=t}$$

$$= v_0^2 e^{-2\gamma t} + \frac{\Gamma}{2\gamma}(1 - e^{-2\gamma t}).$$

$$\boxed{\langle v(t)^2\rangle = v_0^2 e^{-2\gamma t} + \frac{\Gamma}{2\gamma}\left(1 - e^{-2\gamma t}\right)}$$

Implying that at

- Short times: $\langle v^2\rangle \approx v_0^2$

- Long times: $\langle v^2 \rangle \to \Gamma/(2\gamma)$

At equilibrium, the equipartition theorem gives:

$$\frac{1}{2}m\langle v^2 \rangle = \frac{1}{2}k_B T$$

Using this to identify Γ:

$$\Gamma = 2\gamma k_B T$$

This important result relates the noise strength to the damping and temperature — they have the same microscopic origin (molecular collisions).

9.2.4 Mean-square displacement

We now integrate $v(t)$ again to get position $x(t)$ (with $m = 1$):

Using the result above and substituting $\Gamma = 2\gamma k_B T$, one finds (after integrating twice and some algebra):

$$\langle [x(t) - x_0]^2 \rangle = \frac{(v_0^2 - k_B T)}{\gamma^2}(1 - e^{-\gamma t})^2 + \frac{2k_B T}{\gamma}\left[t - \frac{1 - e^{-\gamma t}}{\gamma}\right]$$

Derivation (non-examinable)

The displacement over time t is

$$\Delta x(t) = x(t) - x(0) = \int_0^t v(t_1)\, dt_1.$$

Hence, the mean-squared displacement (MSD) is

$$\langle \Delta x^2(t) \rangle = \left\langle \int_0^t dt_1 \int_0^t dt_2\, v(t_1)v(t_2) \right\rangle.$$

Substituting the expression for $v(t)$ and averaging, we obtain (after some algebra)

$$\langle v(t_1)v(t_2) \rangle = \frac{k_B T}{m}\, e^{-\gamma|t_1 - t_2|}.$$

Inserting this result into the MSD expression gives

$$\langle \Delta x^2(t) \rangle = \frac{2k_B T}{m} \int_0^t dt_1 \int_0^{t_1} dt_2\, e^{-\gamma(t_1 - t_2)}.$$

Evaluating the inner integral first:

$$\int_0^{t_1} e^{-\gamma(t_1-t_2)}\,dt_2 = \frac{1-e^{-\gamma t_1}}{\gamma}.$$

Then the outer integral becomes

$$\int_0^{t} \frac{1-e^{-\gamma t_1}}{\gamma}\,dt_1 = \frac{t}{\gamma} - \frac{1-e^{-\gamma t}}{\gamma^2}.$$

Therefore, the mean-squared displacement is

$$\boxed{\langle \Delta x^2(t)\rangle = 2\frac{k_B T}{m}\left(\frac{t}{\gamma} - \frac{1-e^{-\gamma t}}{\gamma^2}\right) = 2\frac{k_B T}{m\gamma^2}(\gamma t - 1 + e^{-\gamma t}).}$$

Limiting behaviours:

- Short times: ($\gamma t \ll 1$):

  $$\langle [x(t)-x_0]^2\rangle \approx v_0^2 t^2$$

  (correspinding to *ballistic* motion)

- Long time ($\gamma t \gg 1$):

  $$\langle [x(t)-x_0]^2\rangle \approx \frac{2k_B T}{\gamma} t$$

  (corresponding to *diffusive motion*)

why?

To get the short and long time behaviour note that
Short times ($\gamma t \ll 1$):

$$\begin{aligned} e^{-\gamma t} &\approx 1 - \gamma t + \tfrac{1}{2}\gamma^2 t^2 + \cdots, \\ 1 - e^{-\gamma t} &\approx \gamma t - \tfrac{1}{2}\gamma^2 t^2, \\ (1-e^{-\gamma t})^2 &\approx (\gamma t)^2. \end{aligned}$$

Substituting into the MSD expression:

$$\frac{(v_0^2 - k_B T)}{\gamma^2}(1 - e^{-\gamma t})^2 \approx (v_0^2 - k_B T)t^2,$$

$$\frac{2k_B T}{\gamma}\left[t - \frac{1 - e^{-\gamma t}}{\gamma}\right] \approx \frac{2k_B T}{\gamma}\left(\tfrac{1}{2}\gamma t^2\right) = k_B T t^2.$$

Adding both contributions:

$$\boxed{\langle [x(t) - x_0]^2 \rangle \approx v_0^2 t^2,}$$

which corresponds to ballistic motion (distance travelled is proportional to time).
Long times ($\gamma t \gg 1$):

$$e^{-\gamma t} \to 0,$$

$$\frac{(v_0^2 - k_B T)}{\gamma^2}(1 - e^{-\gamma t})^2 \to \frac{(v_0^2 - k_B T)}{\gamma^2},$$

$$\frac{2k_B T}{\gamma}\left[t - \frac{1 - e^{-\gamma t}}{\gamma}\right] \to \frac{2k_B T}{\gamma}\left(t - \frac{1}{\gamma}\right) = \frac{2k_B T}{\gamma}t - \frac{2k_B T}{\gamma^2}.$$

Neglecting constant terms at large t gives:

$$\boxed{\langle [x(t) - x_0]^2 \rangle \simeq \frac{2k_B T}{\gamma}\, t,}$$

which corresponds to *diffusive motion* (distance travelled is proportional to $\sqrt{t}$) with diffusion constant $D = \frac{k_B T}{\gamma}$.

The effective diffusion constant is:

$$D = \frac{k_B T}{\gamma}$$

This is the **Einstein relation**, connecting the rate of diffusion to temperature and damping. It is useful as it allows an explicit expression for the diffusion constant if one knows γ. A famous example is a sphere: the equation for fluid flow past a moving sphere may be solved and yields $\gamma = 6\pi\eta a$ where a is the radius of the sphere and here η is the fluid viscosity. This gives

$$D = \frac{k_B T}{6\pi\eta a}$$

which is the **Stokes-Einstein** formula for the diffusion constant of a colloidal particle.

9.2.5 External Forces and Mobility

Now consider a charged particle with charge q under an external electric field E. The Langevin equation becomes:

$$m\dot{v} = -\gamma v + qE$$

At long times, the particle reaches a steady drift velocity:

$$\langle v \rangle = \frac{qE}{\gamma} = \frac{qED}{k_B T}$$

Defining the mobility μ by $\langle v \rangle = \mu q E$, we get the **Nernst-Einstein relation**:

$$\mu = \frac{D}{k_B T}$$

This relation connects the response of a system to an external perturbation (mobility) with its internal fluctuations (diffusivity).

9.2.6 Molecular Dynamics simulation of Brownian motion for a colloid particle in a liquid suspension

Movies/brownian_colloid.mp4

```
import numpy as np
import matplotlib.pyplot as plt
import matplotlib.animation as animation
from numba import njit

# Parameters
n_fluid = 300
box_size = 20.0
n_steps = 10000
sigma_f = 1.0
sigma_c = 10.0
epsilon = 0.05
mass_f = 1.0
mass_c = 2.0
dt = 1e-5
dt_e = 1e-5
```

```
# Echo the parameter values
print("Simulation Parameters:")
print(f"n_fluid = {n_fluid}")
print(f"box_size = {box_size}")
print(f"n_steps = {n_steps}")
print(f"sigma_f = {sigma_f}")
print(f"sigma_c = {sigma_c}")
print(f"epsilon = {epsilon}")
print(f"mass_f = {mass_f}")
print(f"mass_c = {mass_c}")
print(f"dt = {dt}")

 # Derived quantities

sigma_f6 = sigma_f ** 6
sigma_f12 = sigma_f **12
sigma_cf = 0.5 * (sigma_f + sigma_c)
sigma_cf6 = sigma_cf ** 6
sigma_cf12 = sigma_cf ** 12

np.random.seed(42)

# Safe initialization to avoid overlaps with colloid and other fluid particles
def initialize_fluid_positions(n_fluid, box_size, sigma_f, sigma_c, colloid_pos, min_dist_fa
    min_dist_ff = min_dist_factor * sigma_f
    min_dist_cf = min_dist_factor * 0.5 * (sigma_f + sigma_c)
    positions = []
    max_attempts = 20000

    for _ in range(n_fluid):
        for attempt in range(max_attempts):
            trial = np.random.rand(2) * box_size
            too_close = False

            # Check distance to colloid center
            if np.linalg.norm(trial - colloid_pos[0]) < min_dist_cf:
                too_close = True

            # Check distances to already placed fluid particles
            for existing in positions:
                if np.linalg.norm(trial - existing) < min_dist_ff:
                    too_close = True
```

```
                    break

            if not too_close:
                positions.append(trial)
                break
        else:
            raise RuntimeError("Failed to place a fluid particle without overlap after many a

    return np.array(positions)

colloid_pos = np.array([[box_size / 2, box_size / 2]])
fluid_pos = initialize_fluid_positions(n_fluid, box_size, sigma_f, sigma_c, colloid_pos)
fluid_vel = (np.random.rand(n_fluid, 2) - 0.5)
colloid_vel = np.zeros((1, 2))

@njit
def compute_forces_numba(fluid_pos, colloid_pos, sigma_cf6, sigma_cf12, sigma_f6, sigma_f12,
    forces_f = np.zeros_like(fluid_pos)
    force_c = np.zeros_like(colloid_pos)

    for i in range(n_fluid):
        # Fluid-colloid interaction
        rij = fluid_pos[i] - colloid_pos[0]
        rij -= box_size * np.round(rij / box_size)
        dist2 = np.dot(rij, rij)
        if dist2 < (2.5 ** 2) * ((sigma_cf6 ** (1/6)) ** 2) and dist2 > 1e-10:
            r2 = dist2
            r6 = r2 ** 3
            r12 = r6 ** 2
            fmag = 48 * epsilon * ((sigma_cf12 / r12) - 0.5 * (sigma_cf6 / r6)) / r2
            fvec = fmag * rij
            forces_f[i] += fvec
            force_c[0] -= fvec

        for j in range(i + 1, n_fluid):
            rij = fluid_pos[i] - fluid_pos[j]
            rij -= box_size * np.round(rij / box_size)
            dist2 = np.dot(rij, rij)
            if dist2 < (2.5 ** 2) * ((sigma_f6 ** (1/6)) ** 2) and dist2 > 1e-10:
                r2 = dist2
                r6 = r2 ** 3
                r12 = r6 ** 2
```

```
                fmag = 48 * epsilon * ((sigma_f12 / r12) - 0.5 * (sigma_f6 / r6)) / r2
                fvec = fmag * rij
                forces_f[i] += fvec
                forces_f[j] -= fvec

    return forces_f, force_c

    fluid_history = []
colloid_history = []
forces_f, force_c = compute_forces_numba(fluid_pos, colloid_pos, sigma_cf6, sigma_cf12, sigma

n_equilibration = 2000  # Number of steps to equilibrate before tracking

# Equilibration phase (no history recorded)

for step in range(n_equilibration):
    fluid_pos += fluid_vel * dt_e + 0.5 * forces_f / mass_f * dt**2
    colloid_pos += colloid_vel * dt_e + 0.5 * force_c / mass_c * dt**2
    fluid_pos %= box_size
    colloid_pos %= box_size
    new_forces_f, new_force_c = compute_forces_numba(fluid_pos, colloid_pos, sigma_cf6, sigma
    fluid_vel += 0.5 * (forces_f + new_forces_f) / mass_f * dt_e
    colloid_vel += 0.5 * (force_c + new_force_c) / mass_c * dt_e
    forces_f = new_forces_f
    force_c = new_force_c
    # if step < 10:  # Log only the first few steps
    #     force_mag = np.linalg.norm(force_c[0])
    #     print(f"Step {step:3d} | Colloid Pos: {colloid_pos[0]} | Vel: {colloid_vel[0]} | |

# Production phase (history recorded)

for step in range(n_steps):
    fluid_pos += fluid_vel * dt + 0.5 * forces_f / mass_f * dt**2
    colloid_pos += colloid_vel * dt + 0.5 * force_c / mass_c * dt**2
    fluid_pos %= box_size
    colloid_pos %= box_size
    new_forces_f, new_force_c = compute_forces_numba(fluid_pos, colloid_pos, sigma_cf6, sigma
    fluid_vel += 0.5 * (forces_f + new_forces_f) / mass_f * dt
    colloid_vel += 0.5 * (force_c + new_force_c) / mass_c * dt
    forces_f = new_forces_f
    force_c = new_force_c
    if step % 10 == 0:
```

```
        fluid_history.append(fluid_pos.copy())
        colloid_history.append(colloid_pos.copy())

fig, ax = plt.subplots()
# Calculate figure and plot scale parameters
fig_width_inch = fig.get_size_inches()[0]
dpi = fig.dpi
axis_length_pt = fig_width_inch * dpi
marker_scale = 0.1  # Scale factor for visibility
fluid_marker_size = (marker_scale * axis_length_pt / box_size) ** 2
colloid_marker_size = 0.7*(marker_scale * sigma_c / sigma_f * axis_length_pt / box_size) ** 2
fluid_scatter = ax.scatter([], [], s=fluid_marker_size, c='blue')
colloid_scatter = ax.scatter([], [], s=colloid_marker_size, c='red')
trajectory, = ax.plot([], [], 'r--', linewidth=1, alpha=0.5)
ax.set_xlim(0, box_size)
ax.set_ylim(0, box_size)
ax.set_xticks([])
ax.set_yticks([])
ax.set_xticklabels([])
ax.set_yticklabels([])
ax.set_aspect('equal')
colloid_traj = []

def init():
    empty_offsets = np.empty((0, 2))
    fluid_scatter.set_offsets(empty_offsets)
    colloid_scatter.set_offsets(empty_offsets)
    trajectory.set_data([], [])
    return fluid_scatter, colloid_scatter, trajectory

def update(frame):
    fluid_scatter.set_offsets(fluid_history[frame])
    colloid_scatter.set_offsets(colloid_history[frame])
    colloid_traj.append(colloid_history[frame][0])
    traj_array = np.array(colloid_traj)
    trajectory.set_data(traj_array[:, 0], traj_array[:, 1])
    return fluid_scatter, colloid_scatter, trajectory

ani = animation.FuncAnimation(fig, update, frames=len(fluid_history), init_func=init, blit=Tr
ani.save("brownian_colloid.mp4", writer="ffmpeg", fps=30)
print("Simulation complete. Video saved as 'brownian_colloid.mp4'.")
```

More about the scientists mentioned in this chapter:

Paul Langevin

Robert Brown

Albert Einstein

Walther Nernst

George Stokes

10 Dynamics of first order phase transitions: nucleation, growth and spinodal decomposition

10.1 Introduction to nucleation

In previous discussions, we considered first-order phase transitions but deferred a detailed analysis of the *dynamical* mechanism by which a system evolves from one phase to another. We now address this question explicitly.

Consider again the Ising model at a temperature $T < T_c$, where the system is initially prepared in the majority spin-up phase at zero external field, $H = 0$. At $H = 0$ the spin-up and spin-down phases coexist. We now apply a small negative external field $H < 0$, which lowers the free energy of the spin-down phase relative to the spin-up phase. The spin-down phase is therefore stable, while the spin-up phase is metastable.

It is useful at this point to identify the thermodynamic driving force for the transition. Let

$$\Delta f = f_{\text{meta}} - f_{\text{stable}} > 0$$

be the bulk free-energy density difference between the metastable and stable phases. Converting a volume V of metastable material into the stable phase lowers the bulk free energy by

$$\Delta F_{\text{bulk}} = -V \Delta f.$$

For the Ising model, this free-energy difference is produced by the applied field. Close to coexistence,

$$\Delta f \simeq 2 m_0 |H|,$$

where m_0 is the magnitude of the spontaneous magnetisation. Thus the bulk driving force vanishes as $H \to 0$, where the two phases coexist.

For a molecular system, the same driving force is often expressed in terms of a chemical-potential difference,

$$\Delta\mu = \mu_{\text{meta}} - \mu_{\text{stable}} > 0.$$

The bulk free-energy gain for converting N particles to the stable phase is then approximately

$$\Delta F_{\text{bulk}} \simeq -N\Delta\mu.$$

Thus Δf and $\Delta\mu$ are simply two ways of expressing the bulk thermodynamic driving force, per unit volume or per particle.

Despite the spin-down phase having the lower free energy, the system does not undergo an instantaneous transition. This delay is a consequence of the free-energy barrier associated with nucleating a region of the stable phase within the metastable one, as introduced in Section 5.2. The transition proceeds via *nucleation* of local regions—or *droplets*—of the stable (spin-down) phase embedded in the metastable (spin-up) background. Once nucleated, sufficiently large droplets grow and can ultimately transform the system to the stable phase.

The nucleation of a droplet therefore involves a competition between two contributions to the free energy. There is a bulk free-energy gain, proportional to the volume of the droplet, because the droplet is in the stable phase. This is offset by an interfacial free-energy cost arising from the boundary between the two phases. For the Ising model, broken bonds contribute an energetic cost, while the fluctuating shape of the interface also gives an entropic contribution. Their combined effect is described by the *surface tension* σ.

The competition between the extensive bulk free-energy gain and the sub-extensive interfacial cost gives a free-energy barrier to droplet formation. Only fluctuations that produce a droplet larger than a critical size will grow; smaller droplets will shrink. This is the basis of *classical nucleation theory*.

10.2 Classical Nucleation Theory: Homogeneous Nucleation

We now consider **classical nucleation theory** (CNT) for *homogeneous nucleation*, in which the stable phase nucleates spontaneously in the bulk of the metastable phase, without the aid of impurities, defects or surfaces.

Consider a droplet of the stable (spin-down) phase of radius R embedded in the metastable (spin-up) phase. The change in free energy $\Delta F(R)$ has two contributions:

1. **Bulk free-energy gain**: The stable phase has a lower bulk free-energy density than the metastable phase by $\Delta f > 0$. Thus

$$\Delta F_{\text{bulk}}(R) = -\Delta f \, V_d R^d,$$

   where $V_d R^d$ is the volume of the droplet in d dimensions. For the Ising model, $\Delta f \propto |H|$ close to coexistence. For a molecular system the same contribution can instead be expressed in terms of $\Delta\mu$.

2. **Interfacial free-energy cost**: The boundary between the two phases has area $S_d R^{d-1}$ and carries a free-energy cost proportional to the surface tension σ:

$$\Delta F_{\text{surface}}(R) = \sigma S_d R^{d-1},$$

   where S_d is a geometrical factor (e.g. $S_2 = 2\pi$ in 2D and $S_3 = 4\pi$ in 3D).

The total free-energy change is therefore

$$\Delta F(R) = \sigma S_d R^{d-1} - \Delta f \, V_d R^d.$$

For small droplets the surface term dominates, so increasing the droplet size raises the free energy. For sufficiently large droplets the bulk term dominates and further growth lowers the free energy. The resulting free-energy barrier is shown schematically in Figure 10.1.

The maximum occurs at the critical droplet radius R_c, obtained from

$$\frac{d\Delta F}{dR} = 0,$$

which gives

$$R_c = \frac{(d-1)\sigma S_d}{d\Delta f V_d}.$$

Droplets with $R < R_c$ lower their free energy by shrinking, whereas droplets with $R > R_c$ lower it by growing.

The corresponding nucleation barrier is

$$\Delta F_c = \Delta F(R_c) = \frac{(d-1)^{d-1}}{d^d} \frac{(S_d)^d \sigma^d}{(\Delta f)^{d-1} (V_d)^{d-1}}.$$

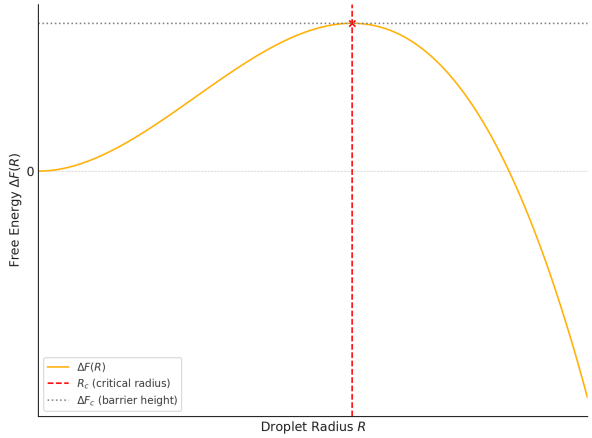


Figure 10.1: Free-energy barrier $\Delta F(R)$ for nucleation of a spherical droplet as a function of radius R (schematic)

This barrier must be surmounted by thermal fluctuations in order for a critical nucleus to form and grow. The nucleation rate per unit volume is, in the Arrhenius approximation,

$$I \sim I_0 \exp\left(-\frac{\Delta F_c}{k_B T}\right),$$

where I_0 is a prefactor determined by microscopic kinetics.

10.2.1 Interpretation and Scaling Behaviour

Several key features follow immediately:

- **Critical radius**: $R_c \sim \sigma/\Delta f$, so the critical droplet becomes very large as $\Delta f \to 0$.
- **Barrier height**: $\Delta F_c \sim \sigma^d/(\Delta f)^{d-1}$, so the nucleation barrier also grows strongly as coexistence is approached.
- **Moving away from coexistence**: Increasing the bulk driving force Δf (or equivalently $\Delta\mu$) reduces both R_c and the barrier, making nucleation easier.

Thus homogeneous nucleation is governed by a competition between the bulk thermodynamic driving force and the interfacial free-energy cost. Close to coexistence the bulk driving force is weak and nucleation can be extremely slow.

10.3 Domain growth

Once a droplet is larger than R_c, further growth lowers the free energy. During this stage the bulk free-energy difference between the metastable and stable phases continues to drive the transformation.

Growth rates depend on the microscopic dynamics: for example, on how rapidly atoms, molecules or spins can rearrange, and on how rapidly material can be transported to the growing phase.

At later times the situation is rather different. The interiors of the domains are then already close to their equilibrium bulk states, and the remaining excess free energy is mainly associated with interfaces. The system then *coarsens* so as to reduce the amount of interface.

It is useful to distinguish these two driving forces:

- nucleation and early growth are driven by the **bulk free-energy difference** between metastable and stable phases;
- late-stage coarsening is driven mainly by the reduction of **interfacial free energy**.

10.4 Spinodal decomposition

So far we have considered a state point just inside the coexistence region, where the original phase remains metastable. The system must then wait for a sufficiently large fluctuation to create a critical nucleus.

Now imagine moving much farther into the coexistence region, as illustrated in Figure 10.2, until the metastable minimum in the free energy disappears. The original phase is then *unstable* rather than metastable. There is no nucleation barrier: small fluctuations can lower the free energy and begin to grow throughout the system. These growing fluctuations develop into regions rich in each of the two equilibrium phases, producing a domain pattern. At later times the domains coarsen: small domains disappear and the typical domain size increases. This process is called *spinodal decomposition*.

If $F(Q)$ is the free energy as a function of an order parameter Q, the spinodal occurs when the metastable minimum merges with the neighbouring maximum. Thus

$$\frac{\partial F}{\partial Q} = 0, \qquad \frac{\partial^2 F}{\partial Q^2} = 0.$$

Inside the unstable region the curvature of the free energy is negative, so small fluctuations can grow rather than having to cross a nucleation barrier.

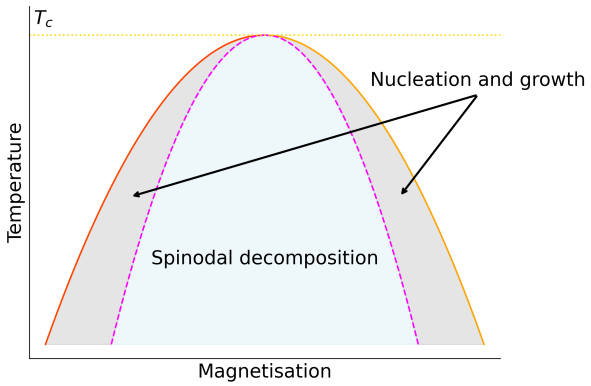


Figure 10.2: Schematic phase diagram for a magnet showing the regions in which one observes nucleation and growth, or spinodal decomposition

After either nucleation and growth or spinodal decomposition, the system generally enters a late-time coarsening regime. The nature of this coarsening depends strongly on whether the order parameter is conserved.

10.4.1 Non-Conserved Order Parameter Dynamics (Model A)

In systems with a non-conserved order parameter, such as the Ising model with single-spin-flip (Glauber) dynamics, the order parameter can relax locally without any conservation constraint. This is called **Model A** dynamics.

The coarse-grained order parameter field $\phi(\mathbf{r}, t)$ evolves so as to reduce the free energy. A simple description is the **Allen–Cahn equation**:

$$\frac{\partial \phi}{\partial t} = -\Gamma \frac{\delta F[\phi]}{\delta \phi},$$

where Γ is a kinetic coefficient. The functional derivative $\delta F/\delta\phi$ is the local thermodynamic driving force for changing the order parameter. Since ϕ is not conserved, the system can lower its free energy by changing ϕ locally.

A simple Ginzburg–Landau free-energy functional is

$$F[\phi] = \int d^d x \left[\frac{1}{2} (\nabla \phi)^2 + V(\phi) \right],$$

with $V(\phi)$ typically a double-well potential such as

$$V(\phi) = \frac{1}{4}(\phi^2 - 1)^2.$$

The squared-gradient term penalises interfaces.

For a curved interface, the reduction of interfacial free energy causes the interface to move. The interface velocity is proportional to its curvature, so for domains of typical size L,

$$v \sim \frac{1}{L}.$$

Thus

$$\frac{dL}{dt} \sim \frac{1}{L},$$

and hence

$$L(t) \sim t^{1/2},$$

corresponding to a dynamic exponent $z = 2$. Small, highly curved domains disappear while the typical domain size grows.

10.4.2 Conserved Order Parameter Dynamics (Model B)

For systems with a conserved order parameter, such as phase separation in binary alloys or the Ising model with spin-swap (Kawasaki) dynamics, the order parameter must be conserved locally. It cannot simply change at a point: material has to be transported from one region to another. This gives **Model B** dynamics.

In this case the functional derivative of the free energy plays the role of a local chemical potential,

$$\mu(\mathbf{r}) = \frac{\delta F[\phi]}{\delta \phi(\mathbf{r})}.$$

Surface tension means that material in a small, highly curved domain has a higher chemical potential than material in a large, more weakly curved domain. This is because small domains have a larger interfacial free-energy cost relative to their volume. Since the curvature of a domain of size L is of order $1/L$, the resulting chemical-potential difference scales as

$$\Delta\mu \sim \frac{\sigma}{L}.$$

This is a curvature-induced chemical-potential difference. It should not be confused with the bulk $\Delta\mu$ introduced earlier as the driving force for nucleation. At late times the bulk phases are already close to coexistence; the remaining driving force comes mainly from interfaces.

Material diffuses down gradients in chemical potential. The flux is therefore

$$\mathbf{J} = -M\nabla\mu,$$

where M is a mobility. Neighbouring domains are typically separated by a distance of order L, so this chemical-potential difference occurs over a distance of the same order. Hence

$$|\nabla\mu| \sim \frac{\Delta\mu}{L} \sim \frac{\sigma}{L^2}.$$

The rate of change of domain size therefore scales as

$$\frac{dL}{dt} \sim \frac{1}{L^2},$$

which gives

$$L(t) \sim t^{1/3}.$$

Thus conserved dynamics coarsen more slowly because growth requires diffusion of material over increasing distances.

The corresponding coarse-grained dynamics are described by the **Cahn–Hilliard equation**:

$$\frac{\partial\phi}{\partial t} = \nabla\cdot(M\nabla\mu) = \nabla\cdot\left[M\nabla\left(\frac{\delta F[\phi]}{\delta\phi}\right)\right].$$

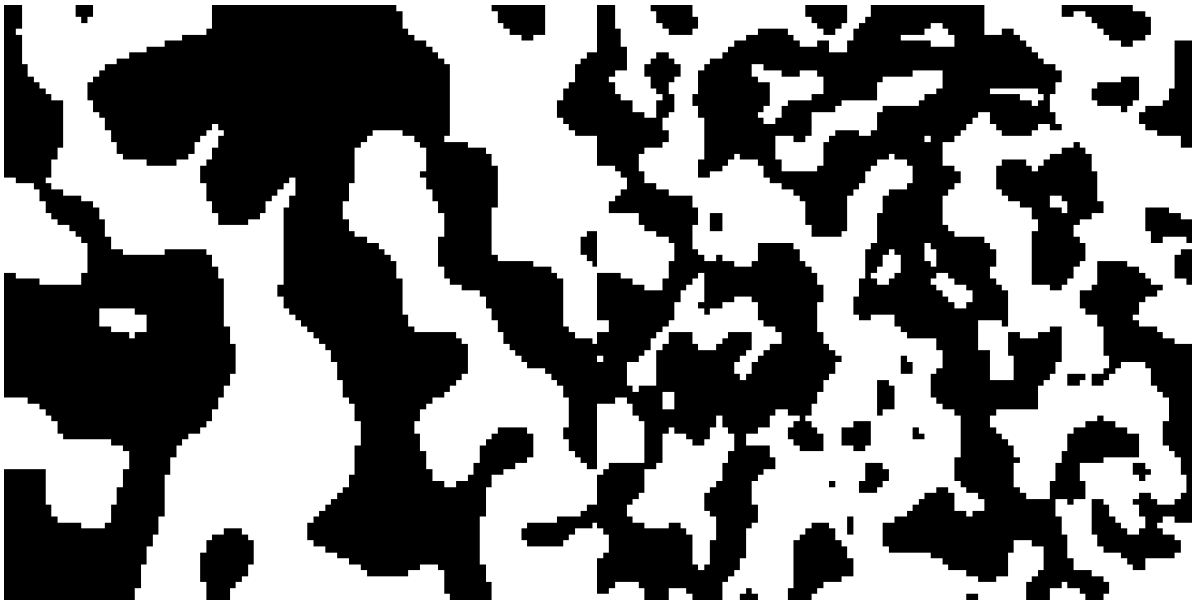
For constant mobility M this reduces to

$$\frac{\partial\phi}{\partial t} = M\nabla^2\left(\frac{\delta F[\phi]}{\delta\phi}\right).$$

10.4.3 Schematic of Domain Growth in 2D Ising model

Here are schematic illustrations of domain growth for:

- Non-conserved dynamics (Model A): Domains coarsen rapidly because the order parameter can relax locally.
- Conserved dynamics (Model B): Coarsening is slower because material has to be transported between domains.



(a) Non-Conserved Dynamics (Model A) (b) Conserved Dynamics (Model B)

Figure 10.3: Schematic illustrations of domain morphology resulting from spinodal decomposition or late-time domain growth for non-conserved and conserved dynamics.

10.4.4 Dynamic Scaling Hypothesis

At late times, both conserved and non-conserved systems exhibit dynamic scaling: the statistical properties of the domain morphology become self-similar under rescaling of lengths by $L(t)$.

For example, the equal-time two-point correlation function satisfies

$$C(r,t) = f\left(\frac{r}{L(t)}\right),$$

where $f(x)$ is a time-independent scaling function. Plots of $C(r,t)$ collapse when plotted as a function of $r/L(t)$.

The structure factor $S(k,t)$, which is the Fourier transform of the correlation function, is experimentally accessible, for example via X-ray or neutron scattering, and also obeys dynamic scaling:

$$S(k,t) = \int d^d r \, e^{-i\vec{k}\cdot\vec{r}} \, C(r,t).$$

Substituting the scaling form of $C(r,t)$ into this expression, and changing variables to $\vec{u} = \vec{r}/L(t)$, gives

$$S(k,t) = L(t)^d \int d^d u \, e^{-i\vec{k}\cdot L(t)\vec{u}} f(u) = L(t)^d g(kL(t)),$$

with $g(x)$ a scaling function.

10.4.5 Summary of Growth Laws

Dynamics Type	Conservation	Equation Type	Growth Law	Dynamic Exponent
Model A (e.g. Glauber)	No	Allen–Cahn	$L(t) \sim t^{1/2}$	$z = 2$
Model B (e.g. Kawasaki)	Yes	Cahn–Hilliard	$L(t) \sim t^{1/3}$	$z = 3$

Remarks:

The domain-growth exponents $1/z$ are robust under many conditions, but can be modified in the presence of disorder, long-range interactions or hydrodynamic effects.

In Model A the system can ultimately reach a uniform equilibrium phase because the order parameter is not conserved. In Model B the overall composition is fixed, so the equilibrium state will in general still contain both phases if the mean composition lies inside the two-phase region.

The approach to equilibrium is algebraically slow because coarsening involves structures on an ever-increasing length scale.

More about the scientists mentioned in this chapter:

John Cahn

Tools for understanding complex disordered matter

Complex disordered systems are composed of an enormous number of interacting components—typically on the order of $\sim 10^{23}$. These interactions can lead to fascinating emergent behaviour, but they also render the systems analytically intractable; it is clearly impossible to solve Newton's equations for such vast numbers of particles. To address this difficulty, we turn to Statistical Mechanics, which you first encountered in your second year. Statistical Mechanics provides the essential framework for connecting the microscopic behaviour of individual constituents with the macroscopic thermodynamic and dynamical properties of the system as a whole.

In this section, we will revisit and expand upon key concepts relevant to our discussion, with particular emphasis on the **free energy**—a central quantity that captures the balance between energy minimisation and entropy maximisation in determining the system's equilibrium state. If any of these ideas feel unfamiliar, you may find it useful to revise the Statistical Mechanics material from your Year 2 *Thermal Physics* course notes.

Ensembles and free energies

Statistical mechanics can be formulated in a variety of ensembles reflecting the relationship between the system and its environment. In what follows we summarise the formalism, focussing on the case of a particle fluid. Analogous equations apply to lattice spin models (see lectures and the book by Yeomans). Key ensembles are:

Microcanonical ensemble

Applies to a system of N particles (or spins) in a fixed volume V having adiabatic walls so that the internal energy E is constant. Denoted as constant-NVE. Let Ω be the number of (micro)states having the prescribed energy:

$$\Omega = \sum_{\text{all states having energy E}}$$

Thermodynamically, the states favored in the canonical ensemble are those that maximise the entropy:

$$S = k_B \ln \Omega \, .$$

where k_B is Boltzmann's constant The microcanonical ensemble is useful for defining the entropy, but is little used in practice.

Canonical ensemble

Applies to a system of N particles in a fixed volume V and coupled to a heat bath at temperature T. Denoted as constant-NVT. A central quantity is the *partition function*

$$Z_{NVT} = \sum_{\text{all states i}} e^{-\beta E_i}, \qquad \beta = 1/(k_B T) \tag{10.1}$$

which is a weighted sum over the states. The partition function provides the normalisation constant in the probability of finding the system in a given state i.

$$P_i = \frac{e^{-\beta E_i}}{Z_{NVT}}. \tag{10.2}$$

The states favored in the canonical ensemble are those that minimise the free energy:

$$F_{NVT} = -\beta^{-1} \ln Z_{NVT} \, .$$

F_{NVT} is known as the Helmholtz free energy. Thermodynamics also supplies a relation for the Helmholtz free energy:

$$F_{NVT} = E - TS \, ,$$

where E is the average internal energy. In minimising the free energy, the system strikes a compromise between low energy and high entropy. The temperature plays the role of arbiter, favouring high entropy at high T, and low energy at low T. The canonical ensemble is usually used to describe systems such as magnets, or a fluid held at constant volume. It is the ensemble we shall use most in this course.

Grand canonical ensemble

Applies to a system with a variable number of particle in a fixed volume V coupled to both a heat bath at temperature T and a particle reservoir with chemical potential μ (which is the field conjugate to N). Denoted as constant-μVT.

The corresponding partition function is a weighted superset of the canonical one

$$Z_{\mu VT} = \sum_{N=0}^{\infty} e^{\beta \mu N} Z_{NVT}$$

and a state probability analogous to Equation 10.2 holds. One can recast this in a form similar to Equation 10.1:

$$Z_{\mu VT} = \sum_{N=0}^{\infty} \sum_{\text{all states i}} e^{-\beta H_i}, \tag{10.3}$$

where $H_i = E_i - \mu N$ is the form of the Hamiltonian in the grand canonical ensemble.

Statistically, the states favored in the grand canonical ensemble are those that minimise the free energy:

$$F_{\mu VT} = -\beta^{-1} \ln Z_{\mu VT}$$

$F_{\mu VT}$ is known as the grand potential. It can also be derived from thermodynamics, from which one finds

$$F_{\mu VT} = E - TS - \mu N = -pV,$$

where p is the pressure.

The grand canonical ensemble is usually used to describe systems such as fluid connected to a particle reservoir. Sometimes for a magnet we consider the effects of an applied magnetic field, which is analogous to working in the grand canonical ensemble: the magnetic field (which is conjugate to the magnetisation) plays a similar role to the chemical potential in a fluid.

Isothermal-isobaric ensemble

Applies to a system with a fixed number of particles N that is coupled to a heat bath at temperature T and a reservoir that exerts a constant pressure p which allows the sample volume to fluctuate. Denoted as constant-NpT.

The corresponding partition function is a weighted superset of the canonical one

$$Z_{NpT} = \int_0^\infty dV e^{-\beta pV} Z_{NVT}$$

or

$$Z_{NpT} = \int_0^\infty dV \sum_{\mathrm{i}} e^{-\beta H_i}, \tag{10.4}$$

where $H_i = E_i + pV$ is the form of the Hamiltonian in the constant-NpT ensemble. Again a state probability analogous to Equation 10.2 holds.

Statistically, the states favored in the constant-NpT ensemble are those that minimise the free energy:

$$F_{NpT} = -\beta^{-1} \ln Z_{NpT}$$

F_{NpT} is known as the *Gibb's free energy* (often denoted G). It can also be derived from thermodynamics, from which one finds

$$F_{NpT} = E - TS + pV = \mu N$$

The constant-NpT ensemble is usually used to describe systems such as a fluid subject to a variable pressure, or a magnet coupled to a magnetic field H. In the latter case the quantity HM plays the role of pV and

$$F_{NpT} = E - TS - MH \,,$$

with M the total magnetisation.

From free energies to observables

Free energies are not directly observable quantities. However, all physical observables can be expressed in terms of *derivatives* of the free energy. One can derive the appropriate relations either from Thermodynamics, or the corresponding statistical mechanics (Revise your year-2 Thermal Physics notes on this if necessary). As an example let us consider a fluid in the isothermal-isobaric ensemble for which the appropriate free energy is $F_{NpT} = E - TS + pV$, and where the volume fluctuates in response to the prescribed pressure. We shall seek an expression for the average volume in terms of the free energy. First lets us take the thermodynamic route. Differentiating the free energy and applying the chain rule we have:

$$dF = dE - TdS - sdT + pdV + VdP \,.$$

But from the first law of thermodynamics, $dE = TdS - pdV$, so

$$dF = -SdT + Vdp\,,$$

and rearranging yields

$$V = \left(\frac{\partial F}{\partial p}\right)_T\,.$$

We can now show that this result is consistent with the definition of F_{NpT} in terms of the partition function. Write

$$Z_{NpT} = \int_0^\infty dV e^{-\beta pV} Z_{NVT} = \int_0^\infty dV \sum_{all\ \ states\ \ i} e^{-\beta(pV_i + E_i)}$$

Then

$$\left(\frac{\partial F}{\partial p}\right)_T = -\frac{1}{\beta}\left(\frac{\partial \ln Z_{NpT}}{\partial p}\right)_T \tag{10.5}$$

$$= -\frac{1}{\beta}\frac{1}{Z_{NpT}}\frac{\partial Z_{NpT}}{\partial p} \tag{10.6}$$

$$= -\frac{1}{\beta}\frac{1}{Z_{NpT}}\int_0^\infty dV \int_{\text{all states}} (-\beta V) e^{-\beta(pV+E)} \tag{10.7}$$

$$= \langle V \rangle_T\,. \tag{10.8}$$

where in the last step we have used the fact that the probability of a state is defined to be $e^{-\beta(pV_i+E_i)}/Z_{NpT}$.

Exercise. Repeat these manipulations to find an expression for the mean particle number N in the grand canonical ensemble

Solution

In the grand canonical ensemble (GCE), the relevant free energy is

$$F_{\mu VT} = E - TS - \mu N$$

From the first law of thermodynamics changes in the internal energy are given by:

$$dE = TdS - PdV + \mu dN = TdS + \mu dN$$

where we have used the fact that V is fixed in the GCE, so $dV = 0$.
Differentiating $F_{\mu VT}$:

$$dF_{\mu VT} = dE - TdS - SdT - \mu dN - Nd\mu = -SdT - Nd\mu$$

where for the last equality we have substitued for dE from above.
Thus

$$\left(\frac{\partial F_{\mu VT}}{\partial \mu}\right)_{T,V} = -N \quad \Rightarrow \quad \langle N \rangle = -\left(\frac{\partial F_{\mu VT}}{\partial \mu}\right)_{T,V}$$

Now consider the statistical mechanics route to calculate $\langle N \rangle$:

$$Z_{\mu VT} = \sum_{N=0}^{\infty} \sum_{\text{states}} e^{-\beta(E_{N,i} - \mu N)}$$

The grand potential (now written as $F_{\mu VT}$) is:

$$F_{\mu VT} = -k_B T \ln Z_{\mu VT}$$

We now differentiate:

$$\left(\frac{\partial F_{\mu VT}}{\partial \mu}\right)_{T} = -k_B T \left(\frac{1}{Z}\frac{\partial Z_{\mu VT}}{\partial \mu}\right)$$

From the partition function

$$\frac{\partial Z_{\mu VT}}{\partial \mu} = \sum_{N=0}^{\infty} \sum_{\text{states}} (\beta N)\, e^{-\beta(E_{N,i} - \mu N)}$$

Substitute:

$$\left(\frac{\partial F_{\mu VT}}{\partial \mu}\right)_{T} = -k_B T \cdot \beta \cdot \frac{1}{Z_{\mu VT}} \sum_{N=0}^{\infty} \sum_{\text{states}} N\, e^{-\beta(E_{N,i} - \mu N)} = -\langle N \rangle$$

where in the last step we have used the fact that in the GCE the Boltzmann probability of a microstate is defined to be $e^{-\beta(E_{N,i} - \mu N)}/Z_{\mu VT}$.